https://doi.org/10.1070/RCR4998

Structural chemistry of host – guest molecular architectures based on mercury-containing macrocycles

Fedor M. Dolgushin,[a, b] Igor L. Eremenko [a, b]

[a] *Kurnakov Institute of General and Inorganic Chemistry of Russian Academy of Sciences, Leninsky prosp. 31, 119991 Moscow, Russian Federation*
[b] *A.N.Nesmeyanov Institute of Organoelement Compounds of Russian Academy of Sciences (INEOS), ul. Vavilova 28, 119991 Moscow, Russian Federation*

Metallomacrocycles that include several metal ions with the Lewis acid properties are peculiar antipodes of crown ethers (referred to as 'anticrowns' in the literature). Recently these architectures have been extensively investigated when searching for efficient and selective anion receptors. In this review, we analyze the data on the molecular and crystal structures of supramolecular complexes of mercury-containing macrocycles (hosts) with anions or neutral nucleophiles (guests). The emphasis is on the identification and systematization of the structure types of complexes in dependence of the guest molecule nature, as well as the macrocycle composition and structure. The factors affecting the selectivity of coordination and competitive ability of various electron donor moieties of guest molecules to binding to the macrocycle are considered. The data in the literature on the nonvalent host – guest and host – host interactions, which are responsible for the formation of molecular complexes and their supramolecular association in crystals, are analyzed. The formulated structural regularities of these coordination compounds with an unusual type of molecular architecture open ways to design directly promising molecular materials on their basis.
The bibliography includes 161 references.

Dedicated to the memory of Professor, Doctor of Chemistry Vladimir Borisovich Shur, whose studies initiated the development of the chemistry of anticrowns in Russia.

Contents

1. Introduction 1493
2. Stereochemical features of mercury(II) compounds 1495
3. Complexes with halide ions 1495
 3.1. Polyanionic chains in the crystal structure of macrocycle **L1** with bromide and iodide ions 1495
 3.2. Sandwich complexes of three-mercury macrocycles **L1** and **LB1** 1496
 3.3. Chain and pyramidal complexes of three-mercury macrocycle **L2** 1497
 3.4. Pyramidal and bipyramidal complexes of four-mercury macrocycles **L3** and **LB2** 1498
 3.5. Bipyramidal complexes of five-mercury macrocycle **L4** 1501
4. Complexes with polyatomic anions 1502
 4.1. Complexes of macrocycle **L1** with linear anions 1503
 4.2. Complexes of macrocycles **L1** and **LB2** with polyhedral dianions $[B_{10}H_{10}]^{2-}$ and $[B_{12}H_{12}]^{2-}$ 1503
 4.3. Complexes of macrocycles **L1**, **LB2**, and **L4** with nitrate and sulfate ions 1505
5. Complexes of macrocycle **L1** with neutral molecules 1507
 5.1. Molecular complexes with neutral Lewis bases 1507
 5.2. Crystalline adducts with aromatic compounds and other conjugated systems 1510
 5.3. Complexes with crown ethers and their heteroanalogues 1513
 5.4. Macrocycle **L1** in coordinating solvents 1514
 5.5. Models of binding macrocycle **L1** to neutral Lewis bases 1514
6. Conclusion 1516
7. List of acronyms and designations 1516

1. Introduction

In recent decades, along with the classical molecular chemistry of covalent bonds, supramolecular chemistry (or, as G.-M. Lehn said,[1] 'chemistry beyond the molecule'), based on intermolecular non-covalent interactions, has been developing very rapidly. Various molecular ensembles, including molecular receptors and their complexes of the host – guest type, are widely used in biotechnology and medicine, catalysis, materials science, and analytical chemistry.[2–5] The main statements of supramolecular chemistry were formulated after discovering (at the end of the 1960s)

F.M.Dolgushin. Doctor of Chemistry, Leading Researcher at the IGIC RAS, Senior Researcher at the INEOS RAS.
E-mail: fedya@ineos.ac.ru
Current research interests: structural chemistry of organometallic and coordination compounds.
I.L.Eremenko. Academician, Doctor of Chemistry, Head of Laboratory at the IGIC RAS and INEOS RAS.
E-mail: ileremenko@yandex.ru
Current research interests: coordination chemistry of polynuclear metal-containing molecules, study of the molecular mechanisms of formation of crystalline supramolecular architectures, search for structure – property relationships.

Translation: Yu.P.Sinkov

Received 21 August 2020

© 2021 Uspekhi Khimii, ZIOC RAS, Russian Academy of Sciences and IOP Publishing Limited

the ability of macrocyclic polyethers (crown ethers and cryptands) to bind selectively cations of alkali and alkaline-earth metals.[6,7] At the same time, when studying the complex formation of halides with macrobicyclic molecules,[8] an inverse problem was formulated: to search for systems capable of recognizing and selective binding of anions. However, for some objective reasons[9] — requirement of large sizes of macrocyclic systems and their instability (because of the enhanced reactivity of electrophilic centres) — the 'non-covalent' coordination chemistry of anions has been developed much more slowly.

The most widespread anion receptors are macrocyclic or cage compounds, for example, protonated cryptands, catapinands, and other macroheterocycles, whose structure provides formation of a complementary system of hydrogen bonds with anion.[10–16]

An alternative type of anion receptors are macrocyclic compounds containing several Lewis acidic atoms, the so-called anticrowns (a term proposed by Professor M.F.Hawthorne *et al.*[17] in 1991 based on the charge-inversion analogy with crown ethers). Anticrowns are characterized by prearrangement of several coordination centres, relatively high strength, and directionality of coordination bonds between the Lewis acid and Lewis base. Additional stabilization of host–guest complexes is obtained due to the macrocyclic and chelating effects. Therefore, anticrowns are promising as efficient and selective anion receptors, and their polydentate properties are of interest from the point of view of activating molecules in organic synthesis and catalysis.

First examples of anticrowns were described for tin-,[18,19] silicon-,[20] and mercury-containing[21] macrocycles. Thereafter diverse metal-containing macrocyclic molecules have been synthesized; many of them exhibit properties of anticrowns, forming complexes with anions and neutral molecules.[22–24] However, the main achievements of the coordination chemistry of anticrowns are related to poly-mercury-containing macrocycles. Of greatest interest are the neutral mercury organic derivatives with coordinatively unsaturated linear C–Hg–C moieties preorganized into a cyclic system for further coordination with guest molecules. There are two types of mercury-containing macrocycles for which systematic studies have been performed:

— mercury atoms are combined into a macrocycle *via* perfluorinated aromatic or aliphatic moieties (macrocycles **L1** – **L4**);

— mercury atoms are combined into a macrocycle *via* carborane moieties (macrocycles **LB1** and **LB2**).

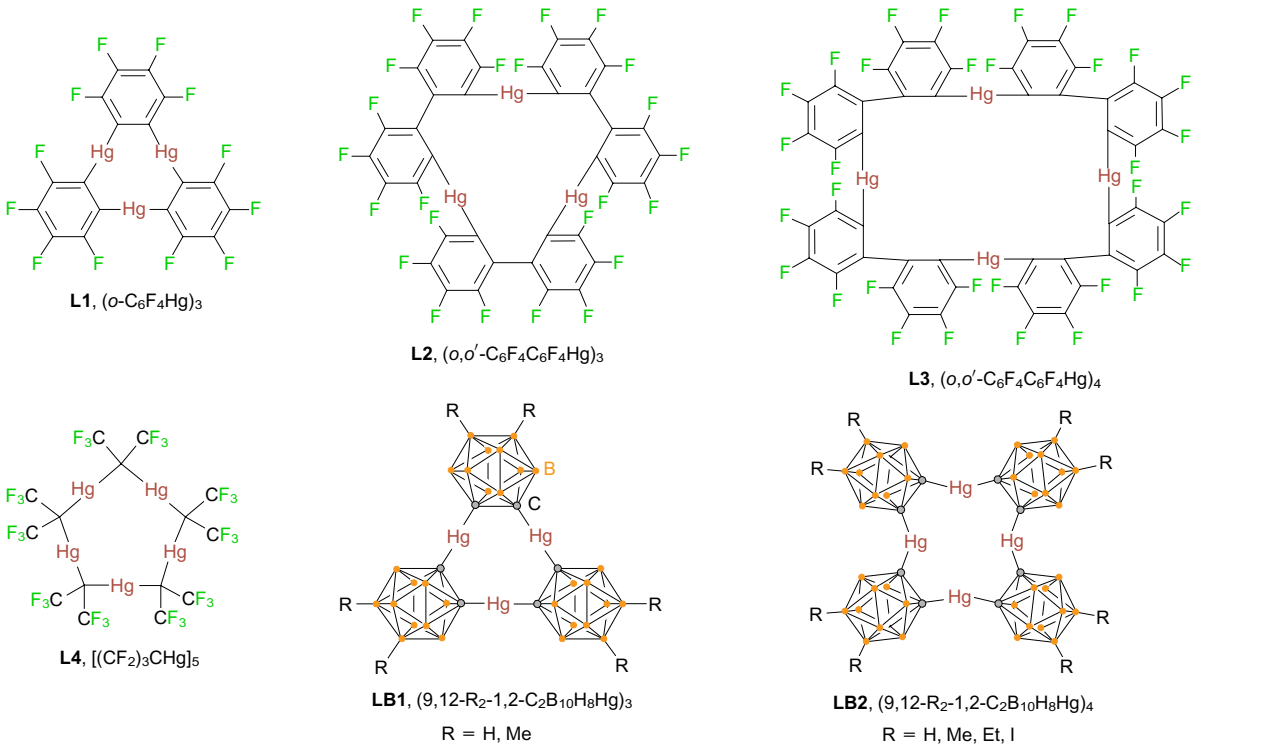
Macrocycles of both types have become classical examples of anticrowns, and they are often mentioned in the publications devoted to the supramolecular chemistry of anion receptors.[10,25–27]

The ability of perfluorinated mercury-containing macrocycles to bind various anions was demonstrated by Professor V.B.Shur *et al.*[28,29] The coordination of guest species to planar macrocycle **L1** is characterized by the absence of steric hindrances, which makes it a convenient model for revealing structural regularities and types of coordination of anions and neutral Lewis bases to anticrowns. Note that 171 structures out of all structurally characterized complexes of host–guest mercury-containing macrocycles [> 200 structures, according to the Cambridge Structural Database (CSD),[30] version 2021] belong to derivatives of macrocycle **L1**.

A synthesis of *o*-carboranylmercury macrocycles **LB1** and **LB2** and study of their properties were performed under the guidance of Professor M.F.Hawthorne.[31–35] The enhanced Lewis acidity of mercury atoms is due to the electron-withdrawing properties of carborane moieties.

Many aspects of the chemistry of mercury-containing anticrowns and their properties have been considered previously.[28,29,35,36] However, comparative analysis and sys-

Structures L1 – L4, LB1, LB2



tematization of the structural data on the molecular and crystal structures of host–guest complexes based on mercury-containing macrocycles have not been performed yet. It is noteworthy that the concept of a 'host–guest complex' accepted in this review implies all types of molecular adducts that contain at least one anticrown molecule and one molecule (or ion) with Lewis base properties, joined by nonvalent intermolecular interactions of the donor–acceptor type.

When preparing this review, we were not aimed at considering all complexes of polymercury-containing macrocycles with anions or neutral Lewis bases for which structural data exist. Our purpose was to reveal types of supramolecular architecture of complexes, search for structural regularities, and describe the geometric and energetic characteristics of the nonvalent interactions implemented between the guest molecule and macrocycle. To this end, we analyzed the data on the molecular and crystal structure of the derivatives (characteristic in our opinion) of primarily the macrocycle **L1**, for which the most representative series of complexes is available in the literature. We will also use some of the structural data on complexes of other polymercury-containing macrocycles to carry out a comparative analysis and, based on the results of this analysis, either extend conclusions to the entire class of compounds, or, *vice versa*, emphasize the distinctive features of a complex, depending on the structure of macrocyclic host molecule.

2. Stereochemical features of mercury(II) compounds

Organic derivatives of divalent mercury are characterized by linear structure of the C–Hg–C moiety, which is explained by the sp-hybridization of the mercury atom. The mercury atom in inorganic and mixed derivatives often has a coordination number (CN) larger than 2, which makes it less accessible for coordination. These and other stereochemical features of mercury compounds were described in detail.[37–42] The mercury atom in organic derivatives is often additionally bound to diverse electron-donating groups. These relatively weak coordination interactions [which are often referred to as secondary bonds, associated with nonvalent (or dispersion) interactions] are implemented at distances greatly exceeding the sum of covalent radii and do not affect the collinearity of covalent Hg–C bonds. According to the CSD,[30] the C–Hg–C bond angle in all structurally characterized organomercury compounds, regardless of the presence and number of additional coordination interactions with the mercury atom, rarely deviate from 180° by more than 10° (Fig. 1). Therefore, the organomercury(II) compounds are relatively weak Lewis acids, which do not form donor–acceptor complexes with a significant charge transfer. In addition, the covalent Hg–C bonds have a pronounced nonpolar character. As a consequence, the contribution of electrostatic interactions with participation of mercury atom is significantly diminished. Therefore, electron-withdrawing substituents (*e.g.*, fluorinated organic ligands) are used to enhance the coordinating properties of organomercury compounds.

The complexes considered below are formed due to the nonvalent interactions between the macrocycle mercury atoms and the electron-saturated parts of the guest molecule (Lewis acid and base, respectively). A descriptive criterion of the presence of these relatively weak interactions in

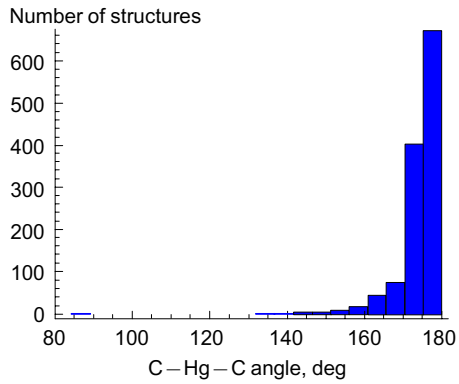


Figure 1. Histogram of C–Hg–C bond angles in organomercury compounds according to the CSD (version of 2021).

crystals are shortened (as compared with the sum of van der Waals radii) interatomic distances.

A standard value is used for the covalent radius (r_{cov}) of mercury atom: 1.30 Å;[37,43] at the same time, a wide range of values has been proposed for its van der Waals radius (R_{vdw}): from 1.5 to 2.1 Å.[37,38,44–46] In our review we accepted the average value: R_{vdw} = 1.75 Å. The choice is based on the results of quantumchemical calculations [using the MP2 and CCSD(T) methods] of the dimer associates of linear molecules HgH_2 and $HgMe_2$, according to which R_{vdw} = 1.75(7) Å.[47] The same value is used to discuss the mercurophilic interactions.[48] The R_{vdw} values for other atoms are taken from Ref. 46 which contains a summary table of radii for all elements.

3. Complexes with halide ions

3.1. Polyanionic chains in the crystal structure of macrocycle L1 with bromide and iodide ions

The complex formation of macrocycle **L1** with halide ions gave products of two compositions, in which according to the elemental analysis data, the macrocycle–halogen ratio was 1 : 1 or 2 : 1. The structure of the 1 : 1 complexes was established by the example of compounds with bromide and iodide ions, which form infinite chains in a crystal $\{[(o\text{-}C_6F_4Hg)_3Hal]_n\}^{n-}$, where Hal = Br or I.[49–51] These results (published in 1991) initiated further development of the coordination chemistry of macrocycle **L1**.

The structure of the polyanionic chain (Fig. 2) in isostructural compounds $[(o\text{-}C_6F_4Hg)_3Hal]^-[PPh_3Me]^+$, where Hal = Br (**1**) or I (**2**), and in $[(o\text{-}C_6F_4Hg)_3Br]^-[PPh_4]^+ \cdot CH_2Br_2$ (**3**) is independent of the counter-ion type or the presence of solvate molecule. The chains were multidecker structures of alternating planar macrocycle molecules and halide ions. Each halogen ion in the chain is bound to six mercury atoms of two neighbouring macrocycles. All Hg–Hal† bond lengths are equalized and amount (on average) to 3.32 Å for Hg–Br⁻ and 3.43 Å for Hg–I⁻. These values are much smaller than the sum of the van der Waals radii of mercury atom and the ionic radius[52] of the corresponding halogen

† A long dash is used in the text to denote interatomic distances and bond lengths, and an ellipsis is used to denote interatomic interactions and intermolecular contacts.

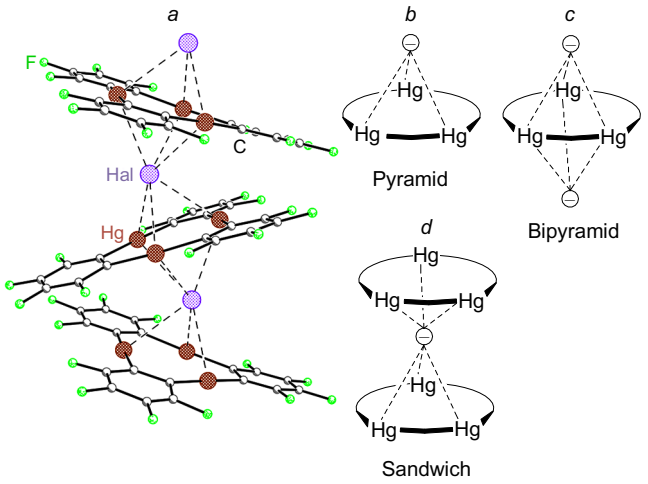


Figure 2. (*a*) Fragment of polyanionic chain $\{[(\mathbf{L1})\mathrm{Hal}]_n\}^{n-}$ (Hal = Br or I) in the crystal structures of multidecker complexes **1**–**3** and (*b*) pyramidal, (*c*) bipyramidal, and (*d*) sandwich moieties in these structures. The distances are Hg–Br^- = 3.245(3)–3.374(3), ⟨3.32⟩ Å; Hg–I^- = 3.331(1)–3.487(1), ⟨3.43⟩ Å. Created by the authors based on the data of Refs 49–51.

($R^{\mathrm{Hg}}_{\mathrm{vdw}} + R^{\mathrm{Br}^-}_{\mathrm{vdw}}$ = 3.71 Å and $R^{\mathrm{Hg}}_{\mathrm{vdw}} + R^{\mathrm{I}^-}_{\mathrm{vdw}}$ = 3.95 Å), but exceed the sum of the corresponding covalent radii ($r^{\mathrm{Hg}}_{\mathrm{cov}} + r^{\mathrm{Br}}_{\mathrm{cov}}$ = 2.52 Å and $r^{\mathrm{Hg}}_{\mathrm{cov}} + r^{\mathrm{I}}_{\mathrm{cov}}$ = 2.71 Å). The neighbouring macrocycles in polyanionic chains are nonparallel, which results in a wedge-like shape of sandwich moieties. Binding to halide ions does not affect the structure of the macrocycles, and the valence environment of mercury atoms in them [the C–Hg–C bond angles (177°) and Hg–C bond lengths (2.08 Å)] coincides with that observed in the structures of four polymorphs of macrocycle **L1** itself.[53, 54]

Structural studies of compounds **1**–**3** demonstrated the ability of perfluorinated mercury-containing macrocycle **L1** to bind halide ions with the formation of supramolecular ensembles of unusual molecular architecture, in which the central complexing species is anion. Formally, the following three moieties can be selected in the multidecker structures of compounds **1**–**3** (Fig. 2 *b*–*d*):

— pyramidal (composition 1 : 1),
— bipyramidal (composition 1 : 2),
— sandwich (composition 2 : 1).

Below we present examples of these complexes, whose composition and structure depend on both the macrocycle structure and the anion nature.

3.2. Sandwich complexes of three-mercury macrocycles L1 and LB1

When interacting with halide ions, the planar three-mercury macrocycle **L1** forms, along with multidecker structures, sandwich complexes of the 2 : 1 composition.[55] The structure of the anion complexes $[(\mathbf{L1})_2\mathrm{Hal}]^-$ [Hal = F (**4**), Cl (**5**), Br (**6**), I (**7**)] is shown in Fig. 3. Each halide ion in sandwich complexes **4**–**7**, as well as in multidecker structures **1**–**3**, is symmetrically bound to six mercury atoms of two macrocycle molecules (the geometric characteristics of these compounds can be compared using the data of Table 1).

The macrocycles in complexes **5**–**7** with chloride, bromide, and iodide ions are nonparallel, which leads to a wedge-shaped structure of sandwich fragments (Fig. 3 *b*). As in multidecker structures **1**–**3**, this structural feature is independent of the cation type and the presence of solvate molecules. The coordination environment of six-coordinate halide ions in wedge-shaped sandwich moieties cannot be described by a regular polyhedron.

The fluoride ion in complex **4** is located between two mutually parallel macrocycles (Fig. 3 *a*). The macrocycle orientation in this complex corresponds to the staggered conformation. The coordination environment of fluoride ion is described by a slightly distorted octahedron with approximately equal Hg–F^- bond lengths, which amount to 2.63 Å; *i.e.*, only slightly exceed the Hg–F bond lengths (2.40 Å) in a mercury(II) fluoride crystal.[56]

The interplanar spacing in sandwich complex **4** is 3.33 Å, with equals distances of 1.665 Å from the fluoride ion to the macrocycle mean planes. An important fact is that the polymorphs of macrocycle **L1** [53, 54] exhibit aggregation of neighbouring molecules into stacking dimers with interplanar spacings of 3.3–3.4 Å. A detailed analysis of the geometric and energetic characteristics of the intermolecular interactions between macrocycles **L1** in the structures of polymorphs of this macrocycle [57] indicates energetic preference of the centrosymmetric stacking dimer, stabilized by the Hg···π interactions between the C–C bonds of the central Hg_3C_6 ring of one macrocycle and the mercury atoms of the other macrocycle. The same mutual arrangement of macrocycles in complex **4** indicates the absence of free space between them, which makes unfavourable their further approach or formation of a wedge-shaped structure.

With an increase in the halide ion size (and, correspondingly, the interplanar spacing), the sandwich complexes in structures **5**–**7** acquire a wedge-shaped configuration. On the assumption of parallel arrangement of macrocycles in these complexes with chloride, bromide, or iodide ions, the interplanar spacings in the sandwiches would be 4.7, 5.0, or

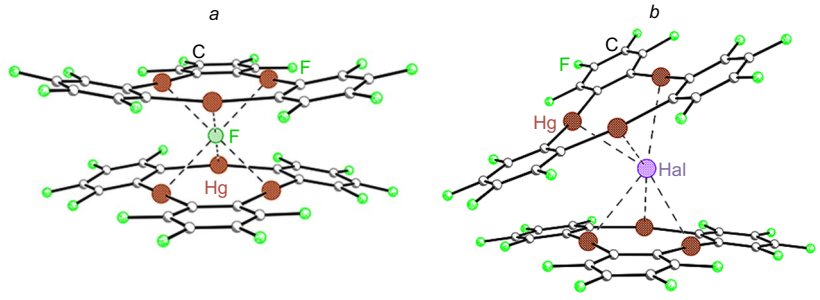


Figure 3. Sandwich complexes of macrocycle **L1** with halide ions. (*a*) Complex with fluoride ion in the structure of $[(\mathbf{L1})_2\mathrm{F}]^-[\mathrm{PPh_4}]^+$ (**4**); the Hg–F^- distances are 2.6140(2)–2.6468(2), ⟨2.63⟩ Å. (*b*) The wedge-shaped sandwich complexes in the structures of $[(\mathbf{L1})_2\mathrm{Cl}]^-[\mathrm{NBu_4}]^+ \cdot 2\,\mathrm{CH_2Br_2}$ (**5**) [the Hg–Cl^- distances are 3.035(3)–3.193(3), ⟨3.10⟩ Å]; $[(\mathbf{L1})_2\mathrm{Br}]^-[\mathrm{NBu_4}]^+ \cdot 2\,\mathrm{CH_2Br_2}$ (**6**) [the Hg–Br^- distances are 3.122(1)–3.323(1), ⟨3.22⟩ Å]; and $[(\mathbf{L1})_2\mathrm{I}]^-[\mathrm{PPh_4}]^+$ (**7**) [the Hg–I^- distances are 3.261(2)–3.410(2), ⟨3.35⟩ Å]. Created by the authors based on the data of Ref. 55.

Table 1. Geometric characteristics of the complexes of macrocycles **L1** and **LB1** with halide ions.

Hal	Sandwich complexes [**L1**···Hal$^-$···**L1**] (see [55])				Sandwich complexes [**LB1**···Hal$^-$···**LB1**] (see [58, 59])				Multidecker complexes [**L1**···Hal$^-$···]$_n$ (see [49–51])			
	Hg–Hal, Å	*d*, Å	ψ, deg	Δ, Å	Hg–Hal, Å	*d*, Å	ψ, deg	Δ, Å	Hg–Hal, Å	*d*, Å	ψ, deg	Δ, Å
F	2.63	1.67	0.0	1.30								
Cl	3.10	2.37	30.6	1.29	3.16	2.45	0.0	1.35				
Br	3.22	2.51	32.6	1.26	3.21	2.49	0.0	1.25	3.32	2.62	34.2	1.36
I	3.35	2.69	31.1	1.15	3.26	2.57	0.0	1.06	3.43	2.74	36.1	1.23

Note. The following designations are used: *d* is the distance from Hal$^-$ to the Hg_3C_6 plane of the macrocycle, ψ is the dihedral angle between the macrocycle planes in a sandwich moiety, and Δ is the difference between the Hg–Hal distance and the ionic radius [52] of the corresponding halide ion (R_F = 1.33 Å, R_{Cl} = 1.81 Å, R_{Br} = 1.96 Å, R_I = 2.20 Å).

5.4 Å, respectively (doubled parameter *d* in Table 1). The wedge-shaped structure of sandwich complexes is stabilized by the dispersion interactions between the closely located groups of macrocycles. Additional stabilization occurs due to the filling of the free space in the wedge open cavity with solvate molecules (in structures **5** and **6**) or phenyl substituents of the counter ion (in structure **7**).[55]

Sandwich complexes with chloride, bromide, or iodide ions were described for the three-mercury macrocycle (9,12-Me_2-1,2-$C_2B_{10}H_8Hg)_3$ (Me_6-**LB1**).[58, 59] The complexes have the same structure (Fig. 4), irrespective of the cation nature and the presence of solvate molecules. In complexes **8**–**10**, *o*-carboranylmercury macrocycles are parallel to each other; the halide ion is located at approximately the same distance from the six mercury atoms, and its coordination environment corresponds to a distorted octahedron. The structure of the complexes and the Hg–Hal bond lengths (see Table 1) are determined by the steric hindrances between the bulk icosahedral moiety in closely located macrocycles. Nevertheless, the attractive Hg···Hal$^-$ interactions in complexes **8**–**10** lead to a decrease in the interplanar spacing between the parallel Hg_3 cores with a decrease in the halide ion radius:[35] I^- (4.90 Å) > Br^- (4.76 Å) > Cl^- (4.67 Å).

Macrocycles **L1** and **LB1** contain an identical central nine-membered Hg_3C_6 ring, which has a planar structure with intramolecular Hg–Hg distances equal to 3.63 Å in **L1** (Refs 53, 54) and 3.73 Å in **LB1**.[60] The distances from the macrocycle centroid to the mercury atoms are 2.10 Å in **L1** and 2.16 Å in **LB1**. The structural similarity of the central part of the macrocycles leads to the formation of the same type of sandwich complexes with halide ions. The steric differences in the structure of the macrocycle peripheral part determine the structural features of the complexes that are related to the mutual arrangement of macrocycles in the parallel or wedge-shaped geometry.

According to Pearson's hard–soft acid–base theory,[61] one would expect the Hg···Hal$^-$ interaction would become more favourable with increasing halogen atomic number. This tendency manifests itself in the structure of complexes **4**–**7**. The increase in the contribution of the covalent component of Hg···Hal$^-$ interaction when passing from F^- to I^- manifests itself in the reduced difference between the contact length and the ionic radius of the corresponding halogen (the parameter Δ in Table 1). This conclusion is consistent with the mass-spectrometry data on the enhanced stability of halide complexes of macrocycle **L1** in the same sequence of halogens;[62] it is also confirmed by the downfield shift of mercury signal in the ^{199}Hg NMR spectrum in solution as a result of the formation of complexes with halide ions, as compared with a free macrocycle. When complexing with macrocycle **L1**, the shift δ(Hg) increases in the sequence F < Cl < Br < I.[55] When complexing with macrocycle **LB1**, the δ(Hg) value increases in the sequence Cl < Br < I.[58]

3.3. Chain and pyramidal complexes of three-mercury macrocycle L2

A macrocyclic system can be modified in order to increase its internal cavity by changing the length of the bridging groups combining mercury atoms into a ring, for example, using macrocycles **L2** and **L3**, in which mercury atoms are bound by perfluorinated biphenylene moieties. The structure of the macrocycle containing three mercury atoms (*o*,*o*′-$C_6F_4C_6F_4Hg)_3$ (**L2**) (Fig. 5) was determined in the

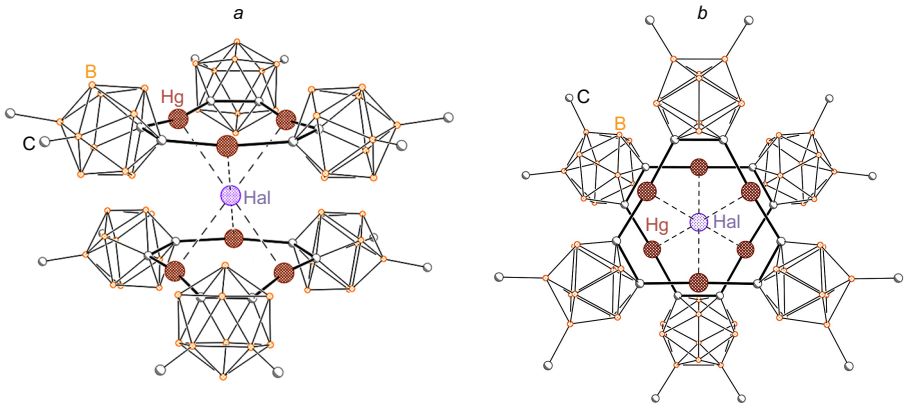


Figure 4. Two projections (*a*, *b*) of the sandwich complexes of hexamethyl-substituted *o*-carboranylmercury macrocycle **LB1** with halide ions: $[(Me_6\text{-}\mathbf{LB1})_2\cdot Cl]^-[PPN]^+$ (**8**), $[(Me_6\text{-}LB1)_2\cdot Br]^-[MePPh_3]^+\cdot 2Me_2CO\cdot 2H_2O$ (**9**), $[(Me_6\text{-}\mathbf{LB1})_2\cdot I]^-[Li\cdot 4(H_2O)]^+\cdot 2MeCN$ (**10**) [PPN is bis(triphenylphosphine)iminium]. Hereinafter the hydrogen atoms are omitted for simplicity. Created by the authors based on the data of Refs 58, 59.

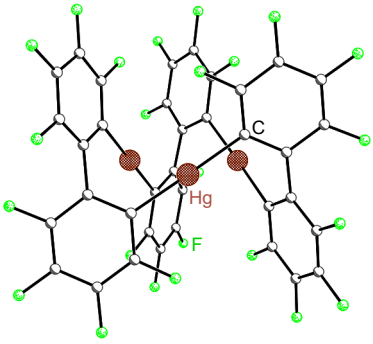


Figure 5. Structure of the macrocycle (o,o'-$C_6F_4C_6F_4Hg)_3$ (**L2**). Created by the authors based on the data of Ref. 63.

structures of neutral adducts with *o*-xylene and acetonitrile.[63]

The central 15-membered Hg_3C_{12} ring in **L2** has a nonplanar structure. Perfluorinated phenylene groups are located above and below the plane passing through the mercury atoms and oriented perpendicular to this plane. The access to the central part of macrocycle cavity is significantly limited because of the formation of a narrow channel for the arriving guest molecule. Note that the cavity size in macrocycle **L2** (the intramolecular Hg — Hg distances are equal to 3.55 Å, the distances from the centroid to the mercury atoms are 2.05 Å) coincide approximately with the corresponding parameters of three-mercury macrocycles **L1** and **LB1**; *i.e.*, an elongation of the organic part does not lead to an increase in the macrocycle cavity. It was also noted [63] that macrocycle **L2** has additional degrees of freedom because of the possibility of aromatic ring rotation in biphenylene fragments. This is a distinction of **L2** from macrocycles **L1** and **LB1** with a conformationally rigid structure. These specific features of the spatial structure of macrocycle **L2** manifest themselves at complexing with halide ions.[64]

The interaction of macrocycle **L2** with salts $[PPh_4]^+Hal^-$ (Hal = Cl, Br, I) gives rise to crystalline compounds $[(\mathbf{L2})Hal]^-[PPh_4]^+ \cdot n(solv)$ (**11** – **13**). The anion complexes in structures **11** – **13** are chains of alternating halide ions and macrocycle molecules (Fig. 6,*a*).

The interaction of macrocycle **L2** with salts $[NBu_4]^+Hal^-$ gives rise to 1 : 1 anionic molecular complexes in $[(\mathbf{L2})Hal]^-[NBu_4]^+ \cdot H_2O$, where Hal = F (**15**), Cl (**16**), Br (**17**). In structures **15** – **17** the η^3-coordinated halide ion is located in the macrocycle cavity and forms a complex of pyramidal structure (Fig. 6 *b*).

Thus, there are two types of complexes of macrocycle **L2** with halide ions in crystals:

— chain structures with external monodentate coordination of anion;

— pyramidal complexes with internal polydentate coordination of anion.

One can suggest that the cooperative type of halide ion binding in pyramidal complexes is thermodynamically preferred over the monodentate coordination in chain structures. The formation of complexes of both types upon interaction with chloride and bromide ions is determined by the kinetic factors of crystallization in the presence of different cations (Table 2). The formation of a pyramidal complex with a iodide ion is apparently sterically unfavourable; thus, a chain structure with external anion coordination is formed, irrespective of the cation type (compounds **13** and **14**). In contrast, a complex with only pyramidal structure (complex **15**) was found for the fluoride ion, which has the smallest size. This selectivity of coordination types for halide ions and macrocycle **L2** indicates that the latter has good prospects for various anion-selective applications.

3.4. Pyramidal and bipyramidal complexes of four-mercury macrocycles L3 and LB2

The structure of macrocycle **LB2** (Fig. 7) is determined in the structure of its neutral adduct with THF,[65] as well as in the structure of the octaethyl-substituted macrocycle with a solvate chloroform molecule.[32] Both these structures lack a

Table 2. Structure types of the complexes formed as a result of the interaction of macrocycle **L2** with the $[PPh_4]^+Hal^-$ and $[NBu_4]^+Hal^-$ salts (according to the data of Ref. 64).

Parameter	F^-	Cl^-	Br^-	I^-
Complexes with $[PPh_4]^+Hal^-$ *salts*				
Structure		Chain	Chain	Chain
Hg — Hal, Å		2.857	2.872	3.179
Complexes with $[NBu_4]^+Hal^-$ *salts*				
Structure	Pyramid	Pyramid	Pyramid	Chain
Hg — Hal, Å	2.505	2.987	3.076	3.174

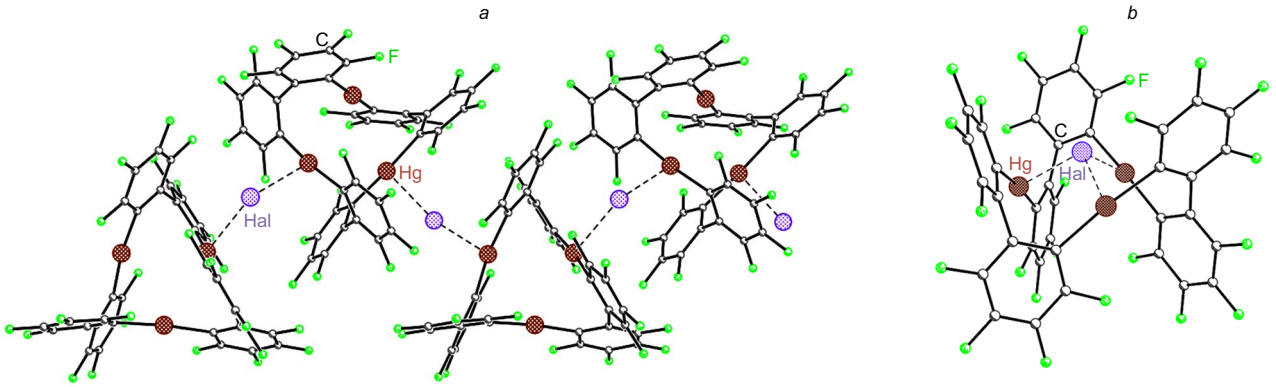


Figure 6. Complexes of macrocycle **L2** with halide ions. (*a*) fragment of the polyanionic chain in the crystal structures of $[(\mathbf{L2})Cl]^-[PPh_4]^+ \cdot CH_2Cl_2$ (**11**), $[(\mathbf{L2})Br]^-[PPh_4]^+ \cdot EtOH \cdot Me_2CO$ (**12**), $[(\mathbf{L2})I]^-[PPh_4]^+$ (**13**), and $[(\mathbf{L2})I]^-[NBu_4]^+$ (**14**); (*b*) pyramidal complexes in the structures of compounds $[(\mathbf{L2})Hal]^-[NBu_4]^+ \cdot H_2O$, where Hal = F (**15**), Cl (**16**), or Br (**17**). Created by the authors based on the data of Ref. 64.

guest molecule in the macrocycle cavity. The central 12-membered Hg_4C_8 ring has an identical bent butterfly-like (saddle) conformation. The proximity of the geometric parameters of macrocycles in these structures to the standard values (the mean values of the bond length and bond angles are, respectively, Hg–C = 2.09 Å and C–Hg–C = 169°, Hg–C–C = 118°) and the absence of strong interactions with the guest molecule suggest that the bent macrocycle conformation corresponds to its equilibrium structure, and the influence of the 9- and 12-substituents of the carborane moieties on the macrocycle structure is minimal. The distances between neighbouring mercury atoms in macrocycles are 3.654–3.775 Å. The distances from the mercury atoms to the centre of four-mercury macrocycle are 2.55–2.65 Å;[32, 65] these values exceed significantly the corresponding distances in the three-mercury macrocycles **L1** (2.10 Å), **LB1** (2.16 Å), and **L2** (2.05 Å).[64]

When studying the complexing of four-mercury macrocycle **LB2** with halide ions, complexes of two types were structurally characterized (Table 3): 1 : 1 complexes, in which the anion is located in the macrocycle cavity, and 1 : 2 complexes, in which two anions are bound to the macrocycle, and a bipyramidal structure is formed (Fig. 8).

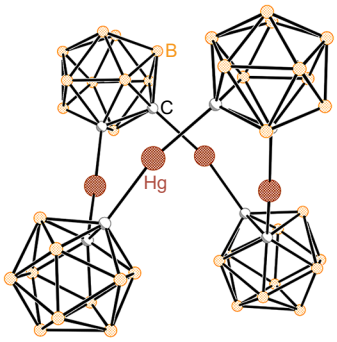


Figure 7. Structure of the unsubstituted four-mercury macrocycle **LB2** in (**LB2**)·4(THF)·2 H_2O. The hydrogen atoms and THF and water solvate molecules are omitted. Created by the authors based on the data of Ref. 65.

Tetrameric *o*-carboranylmercury macrocycles are conformationally nonrigid because of the rotation around the $Hg–C_{carborane}$ bond. The 12-membered Hg_4C_8 ring in complexes with anions may change its conformation from planar to bent, in the form of a butterfly (the angle between the 'butterfly wings' reaches 80°). Apparently, the bent macrocycle conformation is thermodynamically more favourable; it coincides with its uncoordinated form and is characterized by the least deviations of the C–Hg–C and C–C–Hg angles from ideal values: 180° and 120°, respec-

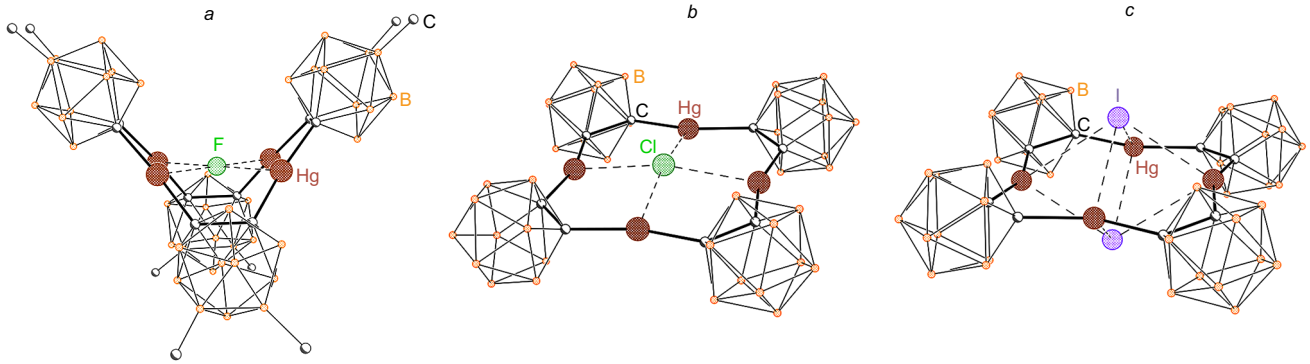


Figure 8. Typical structures of the complexes of tetrameric *o*-carboranylmercury macrocycles with halide ions: (*a*) [(Me$_8$-**LB2**)·F]$^-$[NMe_4]$^+$ (**18**);[66] (*b*) [(**LB2**)·Cl]$^-$[Li]$^+$ (**19**);[17, 32] and (*c*) [(**LB2**)·I_2]$^{2-}$·2[$AsPh_4$]$^+$·2 Me_2CO (**23**).[67] Created by the authors based on the data of the aforementioned studies.

Table 3. Averaged geometric parameters for the complexes of tetrameric *o*-carboranylmercury macrocycles with halide ions.

Anionic complex	Hg–Hal, Å	Macrocycle conformation (see [a])	Hg–Hg, Å (side/ diagonal)	Hal–{Hg4}, Å	C–Hg–C angle, deg	C–C–Hg angle, deg	Ref.
			1 : 1 complexes				
[(Me$_8$-**LB2**)·F]$^-$ (**18**)	2.606	Butterfly (79°)	3.685/5.212	0.00	173.2	119.5	66
[(**LB2**)·Cl]$^-$ (**19**)	2.944	Planar	4.129/5.840	0.38	162.1	126.0	17, 32
[(**LB2**)·Br]$^-$ (**20**)	3.063	Planar	4.104/5.807	0.96	163.0	126.6	32
[(Ph$_4$-**LB2**)·I]$^-$ (**21**)	3.125	Butterfly (146°)	4.051/5.728	1.25	162.3	125.0	68, 69
[(Ph$_4$-**LB2**)·Cl]$^-$ (**22**, three isomers)	2.824	Butterfly (113°)	3.980/5.637	0.14	166.5	123.3	69
			1 : 2 complexes				
[(**LB2**)·2 I]$^{2-}$ (**23**)	3.415	Planar	3.942/5.568	1.96	155.3	123.1	32, 67
[(Me$_8$-**LB2**)·2 I]$^{2-}$ (**24**)	3.421	Planar	3.935/5.561	1.99	155.4	122.9	70
[(Me$_{16}$-**LB2**)·2 I]$^{2-}$ (**25**)	3.395	Planar	3.949/5.585	1.93	155.9	122.9	70
[(I$_8$-**LB2**)·2 I]$^{2-}$ (**26**)	3.362	Planar	3.901/5.515	1.91	154.6	122.4	71
[(Et$_8$-**LB2**)·2 Br]$^{2-}$ (**27**)	3.334	Planar	3.939/5.569	1.83	157.3	123.5	70

[a] The angle between the 'butterfly wings' is given in parentheses for the bent conformation.

tively. The macrocycles in the bent conformation are characterized by the minimum size of internal cavity (see Table 3). In this case, the cavity is optimal for incorporation of a fluoride ion (complex **18**), which is located in the same plane as the four mercury atoms, with the Hg – F distances being 2.5567(5) and 2.6544(6) Å (see Fig. 8 *a*).[66]

The interaction with larger halide ions leads to macrocycle flattening. Apparently, the sharp increase in the ionic radius along the halogen series (when passing from fluorine to chlorine) is critical for preserving the equilibrium macrocycle conformation. The macrocycle flattening leads to an increase in the steric strain and growth of the internal cavity (the transannular Hg – Hg distances increase by 0.5 – 0.6 Å). Due to this, the chloride ion can be located in the macrocycle cavity thus giving 1 : 1 complexes (see Fig. 8 *b*). The chloride ion in complexes **19** and **22** is located almost in plane with the four mercury atoms, and the Hg – Cl distances are, respectively, 2.944(2) Å (Refs 17, 32) and 2.745(4) – 2.896(11) Å.[69] Due to the enlarged size of bromide and iodide ions, 1 : 1 complexes with a pyramidal structure are formed. The deviations of anions from the plane of four mercury atoms in complexes **20** and **21** are, respectively, 0.96 and 1.25 Å (see Table 3 for the parameter Hal – {Hg4}).

Along with the 1 : 1 pyramidal complexes, bromide or iodide ions form unusual complexes of bipyramidal structure and the 1 : 2 composition with the macrocycle **LB2** (see Fig. 8 *c*). Note that the formation of bipyramidal structures with two-anion coordination is not observed for three-mercury macrocycles (including the three-mercury *o*-carboranyl macrocycle **LB1**). One can suggest that the ability of macrocycle **LB2** to bind simultaneously two anions is determined by the presence of four mercury atoms, whose cooperative effect is much stronger than in three-mercury macrocycles.

Bipyramidal dianionic complexes **23** – **27** have the same structure, irrespective of the nature of counter ions ($[AsPh_4]^+$, $[NBu_4]^+$, K^+, Li^+), the presence of solvate molecules and substituents in *o*-carboranes.[32, 67, 70, 71] The central Hg_4C_8 ring of the macrocycle in complexes **23** – **27** has a planar structure; two halide ions are located at both sides of the plane, at identical distances from it, and barely deviate from the axial symmetry of the macrocycle. The largest spread of the Hg – I distances [3.277(1) – 3.774(1) Å] is observed for complex **23**; it is explained by the electrostatic repulsion of two anions, the distance between which [3.969(1) Å] is much smaller than the doubled radius of iodide ion (4.40 Å).[32]

The presence of two anions in bipyramidal complexes **23** – **27** leads to an increase in the Hg – Br and Hg – I bond lengths by 0.25 – 0.30 Å in comparison with the corresponding distances in pyramidal complexes **20** and **21** (see Table 3). At the same time, the Hg – Br and Hg – I bond lengths in bipyramidal complexes **23** – **27** of the four-mercury macrocycle **LB2** coincide in fact with the corresponding bond lengths in multidecker complexes **1** – **3** of the three-mercury macrocycle **L1**, in which bipyramidal moieties can also be selected (see Fig. 2, Table 1).

Thus, the conformational mobility, enlarged cavity size, and larger number of mercury atoms provide structural variety of the complexes of four-mercury macrocycle **LB2** with halide ions: complexes with an anion encapsulated in the macrocycle cavity; 1 : 1 pyramidal complexes; and 1 : 2 bipyramidal complexes, in which two anions are bound to the macrocycle. For comparison, the conformationally rigid three-mercury macrocycle **LB1** forms only sandwich complexes when interacting with halide ions.

The four-mercury macrocycle **L3**, in which mercury atoms are bound by perfluorinated biphenylene groups, was described.[72] The structure of this macrocycle (Fig. 9) was determined in the structures of neutral adducts with *o*-xylene or acetonitrile. The mercury atoms in **L3** lie in a plane, occupying the vertices of slightly distorted parallelogram with sides of 3.39 and 5.28 Å and diagonal distances of 5.27 and 7.12 Å. The perfluorinated phenylene rings are oriented approximately perpendicular to the plane of four mercury atoms and located at both sides of the plane. The size of the transannular cavity in **L3** (the distances from the centroid to the mercury atoms are nonequivalent and amount on average to 2.6 and 3.6 Å) is much larger than that in the three-mercury macrocycle **L2** (2.05 Å); it is comparable with the cavity size in the four-mercury macrocycle **LB2** (2.6 Å). The standard values of the Hg – C bond lengths (2.07 Å) and C – Hg – C bond angles (175°) in **L3** indicate the absence of steric strains during the formation of macrocyclic structure.

Only one complex of macrocycle **L3** with anion was described in the literature: $[(\mathbf{L3})Cl]^-[Li(12\text{-crown-4})_2]^+$ (**28**).[72] Here, the chloride ion is located at the centre of macrocycle cavity, with equivalent Hg – Cl distances; it is lifted by only 0.79 Å above the plane of mercury atoms (Fig. 10). The symmetrically coordinated halide ion contracts the macrocycle, changing its shape from a parallelogram to almost a square [with sides of 3.9195(4) – 4.2219(4) Å]; the C – Hg – C bond angles deviate strongly from the equilibrium value and amount to 167° on average. The macrocycle lability is facilitated by the nonrigidity of biphenylene moiety.[72]

A noteworthy feature is the proximity of the internal-cavity geometric characteristics for the four-mercury macrocycles **LB2** and **L3** in complexes **19** [17, 32] and **28**.[72] The chloride ion coordination in these complexes is in fact the

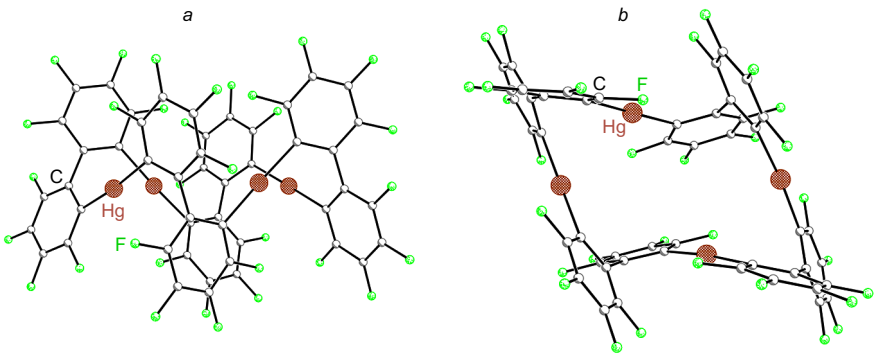


Figure 9. Two projections (*a*, *b*) of macrocycle **L3** in neutral adduct with *o*-xylene (**L3**)·2(*o*-$Me_2C_6H_4$). Created by the authors based on the data of Ref. 72.

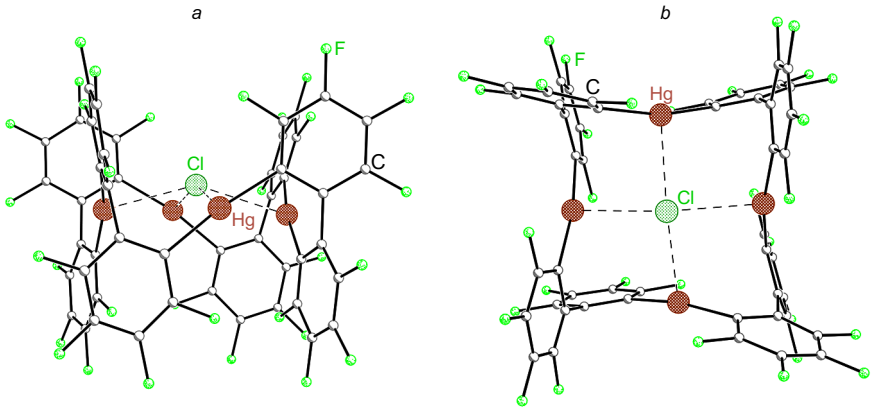


Figure 10. Two projections (*a*, *b*) of the chloride complex of macrocycle **L3** in the structure of $[(\mathbf{L3})Cl]^-[Li(12\text{-crown-}4)_2]^+$ (**28**); Hg–Cl = 2.9221(14)–3.0205(15), ⟨2.96⟩ Å. Created by the authors based on the data of Ref. 72.

same; it is described by a strongly flattened pyramidal structure. Both macrocycles are conformationally mobile. By analogy with the four-mercury *o*-carboranylmercury macrocycle **LB2**, one would suggest the existence of a large variety of structure types of complexes with halide ions for the macrocycle **L3**; they are expected to be obtained in further studies.

3.5. Bipyramidal complexes of five-mercury macrocycle L4

The macrocycle **L4** is the only example of a five-mercury macrocycle with studied anticrown properties.[28, 64, 73, 74]

The structure of macrocycle **L4** was described for a neutral crystal solvate with two water molecules and two pyridine molecules.[75] The central ten-membered Hg_5C_5 ring has a planar structure, and the CF_3 groups are symmetrically located above and below the plane of this ring (Fig. 11 *a*). The undistorted valence environment of mercury atoms (the mean bond angle is C–Hg–C = 176°) and the values of Hg–C bond lengths (2.11 Å) indicate the absence of steric strains during the formation of macrocyclic system. The transannular Hg–Hg distances are 3.312(2)–3.354(2 Å, and the cavity size for the five-mercury macrocycle **L4** (the distance from the centroid to mercury atoms is 2.84 Å) is close to the corresponding characteristics of four-mercury macrocycles **LB2** and **L3**.

The interaction of macrocycle **L4** with the salts $[PPh_4]^+Cl^-$, $[PPh_4]^+Br^-$, or $[PPh_3Me]^+I^-$ gives rise to bipyramidal 1 : 2 complexes in structures **29**–**31** [64, 73, 74] (Fig. 11 *b*). A brief but very illustrative description of these complexes was given by Shur *et al.*[73]: 'The complexes have an unusual shape of a spinning top, the equatorial girdle of which is the mercury-containing metallacycle, whilst the axis direction is fixed by the halide ions located above and below the metallacycle plane at approximately equal distances from the mercury atoms'. Bipyramidal complexes **29**–**31** have anomalously short Hal–Hal distances (Table 4) in comparison with the doubled ionic radius of the corresponding halogens. Obviously, this energetically unfavourable shortening of the distance between two anions is due to the cooperative character of interaction of each halide ion with five mercury atoms of the macrocycle. The Hg–Br and Hg–I bond lengths in bipyramidal complexes **30** and **31** of the five-mercury macrocycle **L4** are close to the corresponding bond lengths in bipyramidal complexes **23**–**27** of the four-mercury macrocycle **LB2** (see Table 3).

Different models have been proposed to describe the binding of halide ions to polymercury-containing macrocycles. For example, the bonds between a halide ion and three mercury atoms of macrocycle can be considered as

Table 4. Geometric parameters of bipyramidal complexes $[(\mathbf{L4})Hal_2]^{2-}$.

Parameter	Cl (**29**) [74]	Br (**30**) [75]	I (**31**) [64]
Hg–Hal, Å	3.089(6)–3.388(8), ⟨3.24⟩	3.229(3)–3.453(3), ⟨3.34⟩	3.396(1)–3.546(1), ⟨3.48⟩
Hal–{Hg5}, Å (see [a])	1.69, 1.56	1.83, 1.79	2.05, 1.99
Hal–Hal, Å	3.25(1)	3.616(5)	4.036(1)
Hg–C, Å	2.05(2)–2.13(1), ⟨2.10⟩	2.04(2)–2.20(3), ⟨2.12⟩	2.09(2)–2.17(2), ⟨2.12⟩
C–Hg–C, deg	172.1(5)–176.1(5), ⟨174.4⟩	170.2(9)–174.5(8), ⟨172.9⟩	173.8(6)–178.0(6), ⟨175.4⟩

[a] Distances from halide ions to the plane of five mercury atoms.

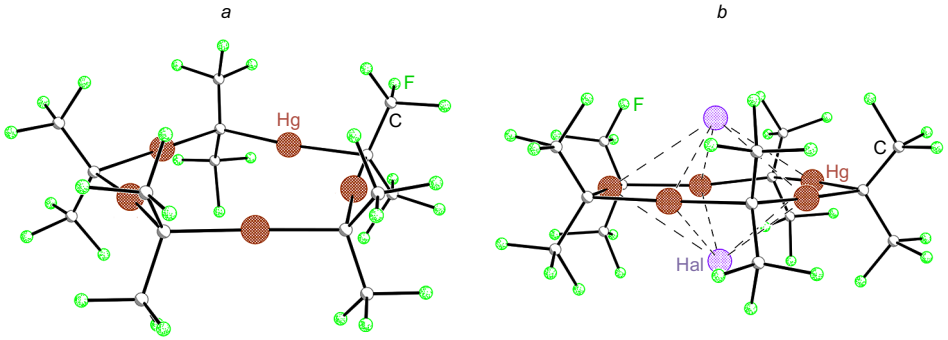


Figure 11. Structures of the (*a*) five-mercury macrocycle **L4** [75] and (*b*) bipyramidal complexes of this macrocycle with halide ions in $[(\mathbf{L4})Cl_2]^{2-}\cdot 2[PPh_4]^+$ (**29**),[73] $[(\mathbf{L4})Br_2]^{2-}\cdot 2[PPh_4]^+$ (**30**),[74] and $[(\mathbf{L4})I_2]^{2-}\cdot 2[PPh_3Me]^+$ (**31**)[64]. Created by the authors based on the data of the aforementioned studies.

donor – acceptor two-centre two-electron interactions between lone electron pairs of the anion and unoccupied orbitals of mercury atoms oriented towards each other. To describe the binding in complexes with four-mercury macrocycles and in complexes with a sandwich structure, a model of three-centre two-electron bonds with participation of unoccupied orbitals of two mercury atoms was suggested.[32, 58, 59, 67]

A description independent of the number of mercury atoms in macrocycle was proposed by analogy with π-complexes of transition metals, for which a model of generalized chemical bonding had been developed.[76] The interaction between the halide ion and macrocycle within this model is described by a headlight-shaped σ-type bond and two two-lobe bonds of the π-type.[77–79] This model can be used to describe pyramidal and bipyramidal complexes, including those formed by the five-mercury macrocycle; however, it is inapplicable to sandwich complexes. The four valence atomic orbitals of the halide ion cannot form generalized chemical bonds (three with each macrocycle). In addition, the results of calculations of sandwich complexes by the MNDO method[79] contradict experimental data, which indicate their symmetric structure.

According to the DFT calculations (TZP-ZORA/TPSS level),[80] the interaction of halide ions with five-mercury macrocycle **L4** in bipyramidal complexes $[(\mathbf{L4})Hal_2]^{2-}$ (Hal = Cl, Br, I) has an electrostatic character. The interactions are 97% determined by the ion – dipole contribution and are characterized by an insignificant (0.13 e) charge transfer from anions to the macrocycle; this charge transfer is the same for the entire halogen series.[80]

The conclusion about the basically Coulomb (ion – dipole) character of interaction between halide ions and polymercury-containing macrocycles is in agreement with the significantly enlarged (in comparison with the sum of covalent radii) Hg – Hal distances and the absence of any significant changes in the valence environment of mercury atoms (the C – Hg – C angles and Hg – C bond lengths retain their standard values).

Summing up the data in the literature on the structure of complexes of polymercury-containing macrocycles with halide ions, we should emphasize the following fundamental issues. All macrocycles are characterized by cooperative (polydentate) binding of halide ion. Depending on the internal size of macrocycle, an anion can either be located at the cavity centre (as in complex **18** of the four-mercury macrocycle **LB2** with a fluoride ion) or be shifted along the symmetry axis of the macrocycle with formation of a pyramidal moiety (which is implemented in all other studied complexes of mercury-containing anticrowns with halide ions). In the latter case, complexes of three structure types can be formed, which differ in the macrocycle-to-halogen stoichiometric ratio: sandwich (2 : 1 composition), pyramidal (1 : 1 composition), and bipyramidal (1 : 2 composition). Along with the steric factors, which determine the coordination availability of mercury centres, or the conformational mobility of some macrocycles, which facilitates more efficient binding of different-size anions, the composition of a complex and the corresponding type of supramolecular architecture are affected by the number of mercury atoms per macrocycle. The total effect of three Lewis acidic centres in three-mercury macrocycles is insufficient for binding more than one anion with the macrocycle; thus, depending on the steric conditions, either sandwich or pyramidal complexes can be formed. The presence of more than three mercury atoms per macrocyclic molecule leads to the formation of bipyramidal structures, in which two anions are bound simultaneously with the macrocycle.

Table 5. Mean values of Hg – Hal bond lengths in the anionic complexes of mercury-containing anticrowns with cooperatively bound halide ions.[64]

Macrocycle	Structure type	Bond length, Å			
		Hg – F	Hg – Cl	Hg – Br	Hg – I
	Three-mercury macrocycles				
L1	Sandwich 2 : 1	2.63	3.10	3.22	3.35
LB1	Sandwich 2 : 1		3.16	3.21	3.26
L2	Pyramid 1 : 1	2.51	2.99	3.08	
	Four-mercury macrocycles				
L3	Pyramid 1 : 1		3.05		
LB2	Pyramid 1 : 1	2.61	2.94	3.06	3.12
LB2	Bipyramid 1 : 2			3.33	3.40
	Five-mercury macrocycle				
L4	Bipyramid 1 : 2		3.24	3.34	3.48

Despite the significant differences in the structure of macrocycles, the Hg – Hal distances in complexes with halide ions have characteristic values, which change systematically with a change in the structure type (Table 5). The smallest distances are observed in pyramidal 1 : 1 complexes, where the anion is bound to three or four mercury atoms of the macrocycle (**L2** or **L3** and **LB2**, respectively). In sandwich complexes with three-mercury macrocycles **L1** and **LB1**, the anion is bound to six mercury atoms, and the Hg – Hal distances are increased by 0.1 – 0.15 Å. The largest Hg – Hal distances are observed in bipyramidal complexes of four- and five-mercury macrocycles (**LB2** and **L4**, respectively), which is explained by the electrostatic repulsion of two anions.

4. Complexes with polyatomic anions

Polymercury-containing anticrowns form complexes not only with monoatomic halide anions but also with various polyatomic anions. In this case, the regularities of the formation of complexes of different structure types, depending on the macrocycle structure, are retained. The largest number of anionic complexes (11 structures, according to the CSD) were characterized for the planar three-mercury macrocycle **L1** (compounds **32** – **42**, Table 6).

Almost all anionic complexes of macrocycle **L1** have a sandwich structure and 2 : 1 composition. There are also multidecker 1 : 1 structures (compound **32**), in which the anion is also located between two mercury-containing macrocycles. Other structure types of anionic complexes (pyramidal or bipyramidal), suggested based on theoretical calculations or existing spectral data for solutions,[89] can barely be found in crystals. The only example of a pyramidal 1 : 1 complex was described for the $[B_{10}H_{10}]^{2-}$ dianion in structure **37**.

The complexing of other mercury-containing macrocycles with polyatomic anions has been poorly studied. A few examples include the complexes of four-mercury macrocycle **LB2** with polyhedral dianion $[B_{10}H_{10}]^{2-}$ (Ref. 87) and nitrate ion,[88] as well as the complex of five-mercury macrocycle **L4** with nitrate ion and doubly charged sulfate ion.[64]

Table 6. Characteristics of complexes of mercury-containing anticrowns with polyatomic anions.

Compound	Composition	Structure type [a]	Hg – Y, Å (see [b])	Ref.
[(**L1**)(SCN)]$^-$ · [NBu$_4$]$^+$ (**32**)	1 : 1	Multidecker sandwich (36.9°)	Hg – S, 3.43	81
[(**L1**)$_2$(BH$_3$CN)]$^-$ [PPN]$^+$ (**33**)	2 : 1	Sandwich (0°)	Hg – N, 2.75 Hg – B, 3.30	82
[(**L1**)$_2$(SO$_4$)]$^{2-}$ · 2 [PhNMe$_3$]$^+$ · 3 EtOH · Me$_2$CO (**34**)	2 : 1	Sandwich (43.3°)	Hg – O, 2.65	83
[(**L1**)$_2$(NO$_3$)]$^-$ · [PPh$_4$]$^+$ (**35**)	2 : 1	Sandwich (34.6°)	Hg – O, 2.93	83
[(**L1**)$_2$(NO$_3$)]$^-$ · [PPN]$^+$ (**36**)	2 : 1	Sandwich (0°)	Hg – O, 2.92	83
[(**L1**)(B$_{10}$H$_{10}$)]$^{2-}$ · 2 [NBu$_4$]$^+$ · MeOH (**37**)	1 : 1	Pyramid	Hg – H, 2.7	84
[(**L1**)$_2$(B$_{10}$H$_{10}$)]$^{2-}$ · 2 [PPN]$^+$ · Et$_2$O (**38**)	2 : 1	Sandwich (20.1°)	Hg – B, 3.36 Hg – H, 2.52 Hg – B, 3.28	84
[(**L1**)$_2$(B$_{12}$H$_{12}$)]$^{2-}$ · 2 [NBu$_4$]$^+$ (**39**)	2 : 1	Sandwich (59.4°)	Hg – H, 2.55	84
[(**L1**)$_2$(B$_{12}$H$_{11}$SCN)]$^{2-}$ · 2 [NBu$_4$]$^+$ (**40**)	2 : 1	Sandwich (50.5°)	Hg – B, 3.31 Hg – H, 2.65 Hg – B, 3.42	85
[(**L1**)$_2$(Fe(CN)$_6$)]$^{3-}$ · 3 [PPN]$^+$ · Et$_2$O · 3 Me$_2$CO (**41**)	2 : 1	Sandwich (11.1°)	Hg – N, 2.79	86
[(**L1**)$_2$(Fe(CN)$_5$NO)]$^{2-}$ · 2 [PPN]$^+$ (**42**)	2 : 1	Sandwich (0°)	Hg – N, 2.94	86
[(Et$_8$-**LB2**)(B$_{10}$H$_{10}$)$_2$]$^{4-}$ · 4 [PMePh$_3$]$^+$ · 2 MeCN (**43**)	1 : 2	Bipyramid	Hg – H, 3.2 Hg – B, 3.54	87
[(**LB2**)(NO$_3$)$_2$ · H$_2$O]$^{2-}$ · 2 [K(18-crown-6]$^+$ · H$_2$O · Me$_2$CO (**44**)	1 : 2	Bipyramid	Hg – O, 2.92	88
[(**LB2**)(NO$_3$)$_2$]$^{2-}$ · 2 [K(18-crown-6]$^+$ (**45**)	1 : 2	Bipyramid	–	88
[(**L4**)(NO$_3$)$_2$]$^{2-}$ · 2 [PPh$_4$]$^+$ (**46**)	1 : 2	Bipyramid	Hg – O, 2.95	64
[(**L4**)SO$_4$]$^{2-}$ · 2 [PPh$_4$]$^+$ · Me$_2$CO · EtOH (**47**)	1 : 1	Pyramid	Hg – O, 2.89	64

[a] The values of the dihedral angle between macrocycle planes (wedge angle) are given in parentheses for sandwich complexes; [b] the distance from the macrocycle mercury atoms to the Y atom of the anion involved in the polydentate η^n-coordination.

These compounds, as well as the complexes of the aforementioned macrocycles with halide ions, are characterized by the formation of bipyramidal 1 : 2 structures, in which two anions are bound to a macrocycle. The structure types of the complexes of mercury-containing macrocycles with polyatomic anions are given in Table 6.

4.1. Complexes of macrocycle L1 with linear anions

Complex **32** of macrocycle **L1** with pseudohalide SCN$^-$ ion in crystal has a structure of a wedge-shaped multidecker sandwich (Fig. 12 *a*),[81] identical to that of polyanionic chains in structures **1** – **3** with bromide and iodide ions (see Fig. 2). The thiocyanate ion is bound to two neighbouring macrocycles *via* a sulfur atom with nonequivalent Hg – S distances. The linear anionic molecule is located in the open part of wedge-shaped sandwich (the wedge angle is 36.9°).

The coordination of thiocyanate ion in complex **32** can be explained by the affinity of mercury and sulfur atoms. However, taking into account the ambiguity of the spectral data obtained in solutions,[81] one cannot completely exclude the possibility of coordination to the CN group. For example, in sandwich complex **33**[82] with cyanoborohydride anion BH$_3$CN$^-$ (Fig. 12 *b*), both anionic groups (cyanide and borohydride) are involved in binding with macrocycles, and the linear anion is oriented perpendicular to the planes of parallel macrocycles. The nitrogen atom of the cyanide group is symmetrically bound to the three mercury atoms of the macrocycle [the Hg – N distances are 2.713(15) – 2.780(14) Å]. The binding of the BH$_3$ group to the macrocycle, presumably *via* three-centre B – H···Hg interactions, is evidenced by shortened Hg – B distances: 3.24(4) – 3.41(4) Å.[82]

Complex **33** with parallel arrangement of macrocycles differs from the sandwich moieties in complexes with thiocyanate (**32**) and halide (**1** – **7**) ions, having a wedge-shaped structure. The parallel arrangement of macrocycles in complexes **1** – **7** would lead to an unfavourable (with respect to the free-space filling) interplanar spacing ~5 Å (see Table 1, doubled parameter *d*). The distance between the macrocycles in complex **33** is 6.88 Å, which allows for incorporation of fragments of neighbouring molecules with intermolecular distances 3.4 – 3.5 Å, characteristic of van der Waals contacts (for example, stacking contacts between aromatic rings). This is confirmed by the crystal packing of compound **33** (Fig. 12 *c*), which consists of alternating anion and cation layers.[82]

4.2. Complexes of macrocycles L1 and LB2 with polyhedral dianions $[B_{10}H_{10}]^{2-}$ and $[B_{12}H_{12}]^{2-}$

The complexes of macrocycles **L1** and **LB2** with polyhedral borane dianions $[B_{10}H_{10}]^{2-}$, $[B_{12}H_{12}]^{2-}$, and $[B_{12}H_{11}SCN]^{2-}$ have been structurally characterized (Fig. 13, see Table 6).[84, 85, 87] Binding to macrocycles is implemented due to the bridging B – H···Hg interactions of two types. In all complexes one of the BH groups is directed towards the macrocycle centre and bound to all mercury atoms (polydentate η^n-coordination). In addition, some polyhedron vertices are bound to macrocycle mercury atoms, one mercury atom per vertice (monodentate η^1-coordination). Under these conditions, the dianion forms a maximally possible number of contacts with electron-deficient mercury atoms of the macrocycle. For example, decaborane $[B_{10}H_{10}]^{2-}$, which has the geometry of two-cap square antiprism (D_{4d} symmetry), is involved in the η^3-coordination of one of the equatorial BH groups in complexes **37** and **38** with the three-mercury macrocycle **L1** (see Fig. 13 *a*,*b*). Two more decaborane vertices are involved in the η^1-coordination. In bipyramidal complex

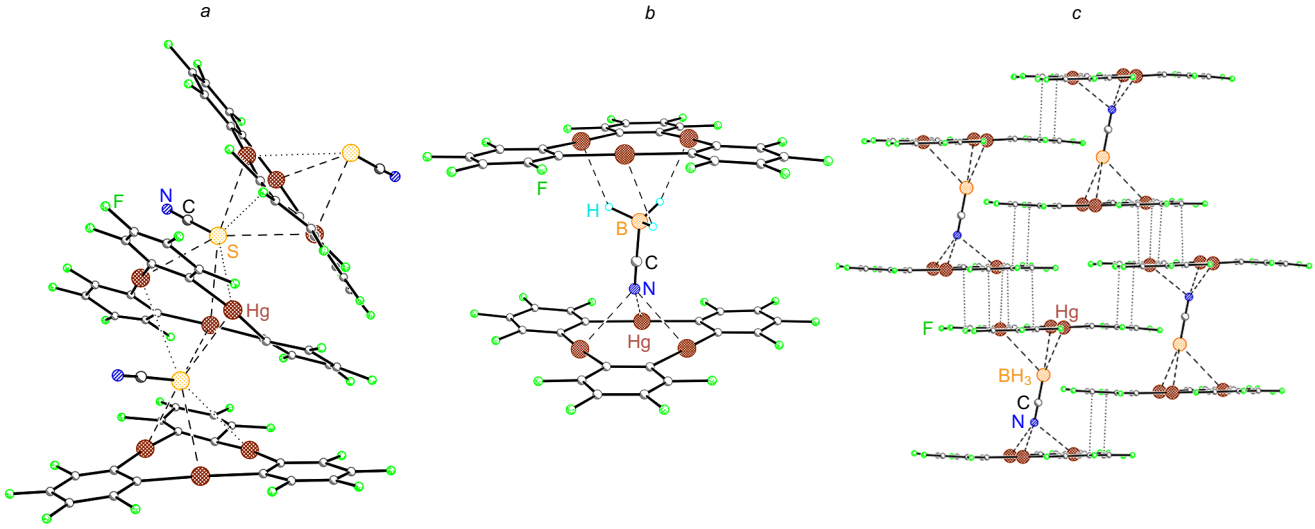


Figure 12. (*a*) Fragment of polyanionic chain in the crystal structure of compound **32**,[81] (*b*) sandwich complex with a cyanoborohydride anion in the structure of compound **33**,[82] and (*c*) mutual arrangement of sandwich complexes in this structure [dotted lines show the shortest intermolecular contacts Hg···π(C) 3.30 – 3.61 Å and π(C)···π(C) 3.32 – 3.46 Å]. Created by the authors based on the data of the aforementioned studies.

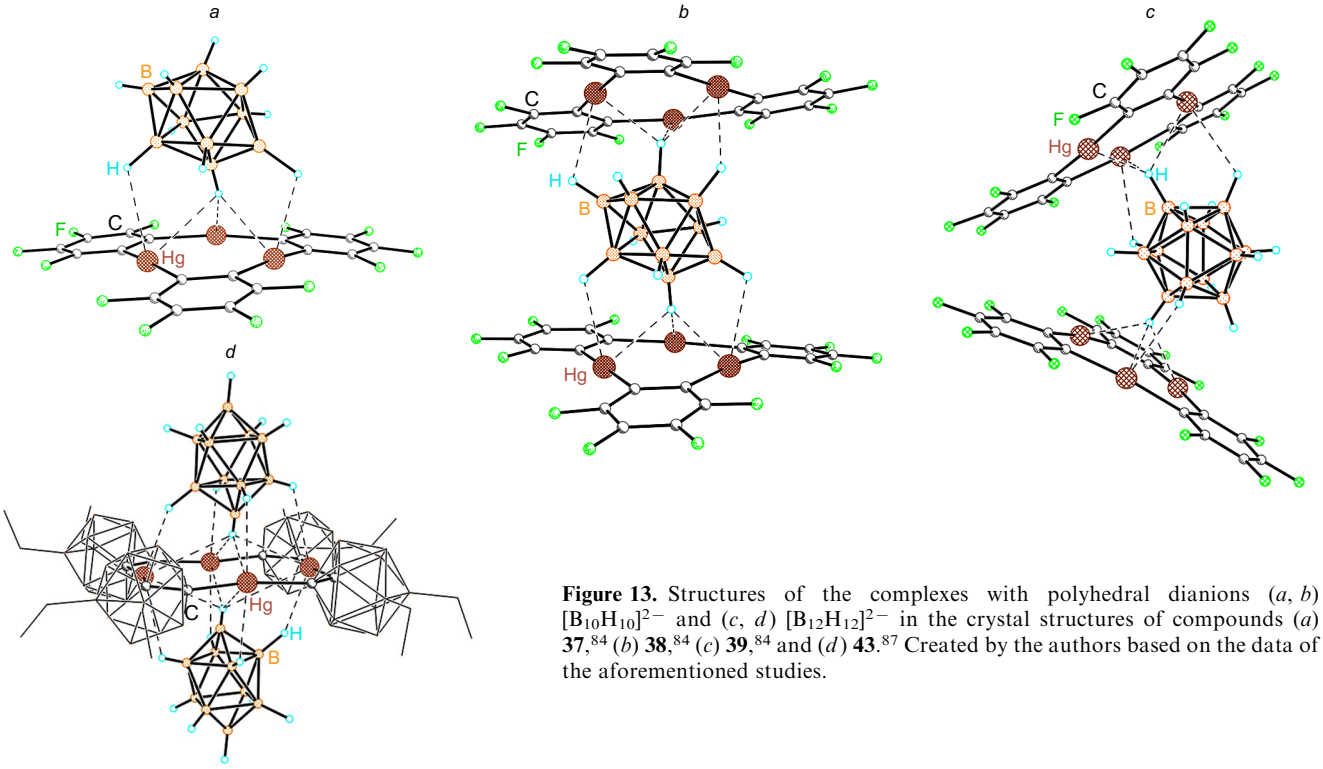


Figure 13. Structures of the complexes with polyhedral dianions (*a*, *b*) $[B_{10}H_{10}]^{2-}$ and (*c*, *d*) $[B_{12}H_{12}]^{2-}$ in the crystal structures of compounds (*a*) **37**,[84] (*b*) **38**,[84] (*c*) **39**,[84] and (*d*) **43**.[87] Created by the authors based on the data of the aforementioned studies.

43 (Fig. 13 *d*) with the four-mercury macrocycle **LB2**, one of apical decaborane vertices is directed towards the macrocycle centre. As a result, an optimal set of monodentate B – H – Hg interactions of four equatorial vertices of each decaborane and four mercury atoms of the macrocycle is implemented. In the case of interaction of macrocycle **LB2** with dodecaborane $[B_{12}H_{12}]^{2-}$, the complex is not formed, which is explained by the lower nucleophilic ability of dodecaborane and incompatibility with respect to the symmetry of icosahedral dianion with the four-mercury macrocycle.[35,87] Complexing of sterically unhindered macrocycle **L1** with dianion $[B_{12}H_{12}]^{2-}$ has been established not only in crystal (compound **39**) but also in solution, as confirmed by the spectral data.[84] The wedge-shaped sandwich complex in structure **39** is characterized by an extraordinary large wedge angle (the dihedral angle between the macrocycle planes is close to 60°). One would suggest that this structural feature of the complex indicates directionality of polydentate interactions, which involve BH groups in *meta*-positions of icosahedron.

In the case of complexing of $[B_{10}H_{10}]^{2-}$, $[B_{12}H_{12}]^{2-}$, and $[B_{12}H_{11}SCN]^{2-}$ dianions with macrocycle **L1**, the

absorption bands that are due to the coordinated BH groups are shifted by 157–200 cm^{-1} relative to the signals from uncoordinated groups in the IR spectra of solutions (THF, THF–acetone).[84,85] This fact not only confirms the complexing of boron hydrides with macrocycle **L1** in solution but also indicates the high strength of B–H···Hg interactions.[90] At the same time, molecular fragments of the complexes retain their retain their structure in the crystal.

The unique ability of mercury-containing anticrowns to bind diverse anion particles was demonstrated by an example of sandwich complexes of macrocycle **L1** with metal-complex hexacyanoferrate(III) and nitroprusside anions (correspondingly, complexes **41** and **42**).[86] In each complex the anion is bound to macrocycles *via* four cyanide groups. The contribution of the Coulomb component to the interaction of anions with macrocycle clearly manifests itself in the decrease in the Hg–N distances in structure **41** with a triply charged anion $[Fe(CN)_6]^{3-}$ as compared to structure **42** with a doubly charged $[Fe(CN)_5NO]^{2-}$ anion (2.79 and 2.94 Å, respectively).[86]

4.3. Complexes of macrocycles L1, LB2, and L4 with nitrate and sulfate ions

Like most anion complexes of macrocycle **L1**, the complexes with sulfate and nitrate ions in **34**–**36** have a sandwich structure (Fig. 14).[83] Being bound to the macrocycles, anions are involved in cooperative interaction (the oxygen atom is η^3-coordinated to three mercury atoms) and additionally bound to one of the mercury atoms (η^1-coordination). The Hg–O bond lengths in the pyramidal moieties corresponding to the η^3-coordination are significantly shortened in the complex with sulfate ion (2.65 Å) as compared with the same bonds in complexes with nitrate ion (2.93 Å).[83] Like in complexes **41** and **42** with metal-complex cyanide anions, the difference is explained by the value of negative charge of the anion guest and the corresponding contribution of electrostatic interaction.

The influence of counter ion on the structure of anion complexes and the ways of their self-organization in crystals were studied by an example of sandwich complexes with a nitrate ion in the presence of $[PPh_4]^+$ in compound **35** and $[PPN]^+$ in compound **36**.[83] The sandwich complex in **35** has a wedge-shaped structure (the wedge angle is 34.6°), whereas in **36** the macrocycles of the sandwich complex are parallel (Figs. 14 *b*,*c*).

Irrespective of the mutual arrangement of macrocycles in sandwich complexes, the Hg–O bond lengths corresponding to η^3-coordination coincide (Table 6). At the same time, in complex **36** with a parallel arrangement of macrocycles, the Hg–O distances corresponding to the monodentate η^1-coordination are much larger [3.137(8) and 3.543(8) Å] than the corresponding distances in wedge-shaped complex **35** [2.885(3) and 2.723(3) Å].[83] Apparently, the shorter contacts are consistent with the more favourable wedge-like shape of sandwich complex.

The thermodynamic preference of wedge-shaped structure is confirmed by the results of quantumchemical calculations (M052X/SDD).[91] Irrespective of the initial structure of sandwich complex with a nitrate ion (wedge-shaped or parallel arrangement of macrocycles), optimization leads to the wedge-shaped sandwich geometry with an angle of 40° between macrocycles.

The general regularity of the crystal structure of anionic sandwich complexes of macrocycle **L1** is that the parallel or close-to-parallel arrangement of macrocycles (wedge angle $<20°$) is implemented in all structures with a $[PPN]^+$ cation. The sandwich complexes in structures with tetrahedral $[NR_4]^+$ or $[PR_4]^+$ cations have a wedge-shaped geometry with a wedge angle $>30°$ (see Table 6).

Anionic sandwich complexes in crystals are combined into stacks. The aggregation of complexes into stacks occurs *via* numerous shortened contacts Hg···C_{arom} and C_{arom}···C_{arom} between the external sides of macrocycles of neighbouring sandwiches. These contacts correspond to the stacking Hg···π and π···π interactions with interplanar spacings of 3.3–3.5 Å.[82–86] The structure of stacks and their packing are identical in different crystal structures; they are determined by only the shape of sandwich complex. Wedge-shaped sandwiches form zigzag stacks (Fig. 15 *a*). These stacks in crystals are shielded from all sides by cations and solvent molecules, whose terminal groups fill the free space in the wedge. Sandwich complexes with parallel macrocycles form staircase stacks (see Figs 12 *c* and 15 *b*). The free space in sandwiches is filled with perfluorophenylene moieties of the macrocycles from neighbouring stacks, which leads to the formation of anion layers.

Among described structures, there are complexes with nitrate ions of tetramer *o*-carboranylmercury macrocycle **LB2**[88] and cyclic pentamer perfluoroisopropylidenemercury **L4**.[64] In contrast to sandwich complexes **35** and **36** of the three-mercury macrocycle **L1**, the complexes of four-

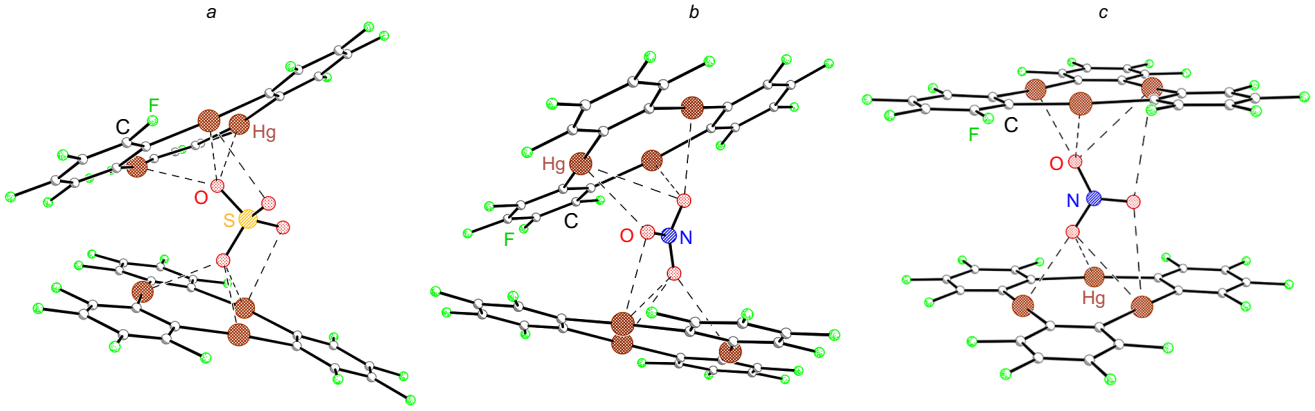


Figure 14. Structure of the sandwich complexes of macrocycle **L1** with (*a*) sulfate and (*b*, *c*) nitrate ions in the crystal structures of compounds (*a*) **34**, (*b*) **35**, and (*c*) **36**. Created by the authors based on the data of Ref. 83.

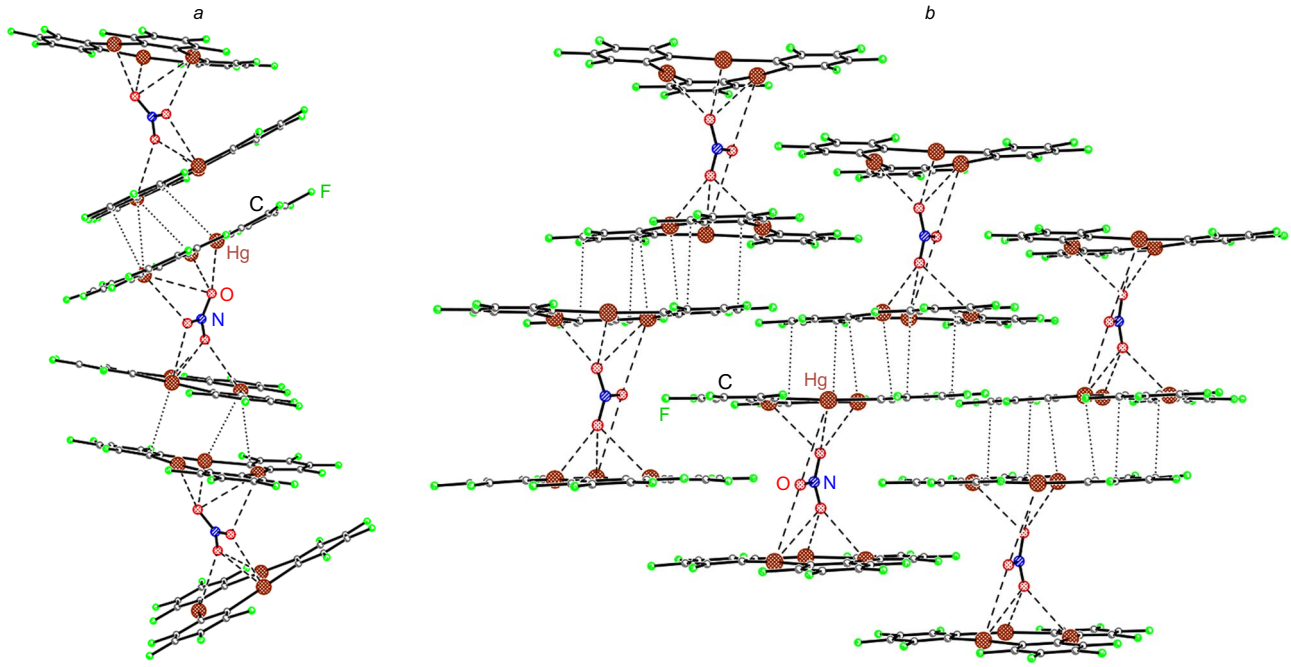


Figure 15. (*a*) Zigzag stack of wedge-shaped sandwich complexes in the structure of compound **35** and (*b*) interpenetrating stacks of sandwich complexes with parallel arrangement of macrocycles in the structure of compound **36**. Created by the authors based on the data of Ref. 83.

or five-mercury macrocycles have a bipyramidal structure (Figs. 16 *a* – *c*), which is in agreement with the behavioural regularities of polymercury-containing macrocycles in complexing with halide ions. A similarity of the coordination of nitrate ion with different macrocycles was noted.[64]

Coordination of doubly charged sulfate ion with the five-mercury macrocycle **L4** leads to the formation of a 1 : 1 complex having a pyramidal structure (Fig. 16 *d*).[64] A specific feature of sulfate ion binding in this complex is the location of one of anion oxygen atoms at the centre of macrocycle cavity, with identical Hg – O distances, equal to 2.843(8) – 2.902(7) Å.

Despite the limited number of examples of complexes of different mercury-containing macrocycles with polyatomic anions, the existing structural data give grounds to draw some general conclusions. Like in complexes with halide ions, the structure of macrocycle (cavity size, conformational rigidity, steric features of substituents) and the number of mercury atoms in it determine the most stable structure types of supramolecular complexes with polyatomic anions: sandwich, pyramid, bipyramid, or anion location in the macrocycle cavity. The main type of anion binding is the polydentate η^n-coordination (cooperative binding). At coordination of anions having several nucleophilic centres, additional monodentate interactions

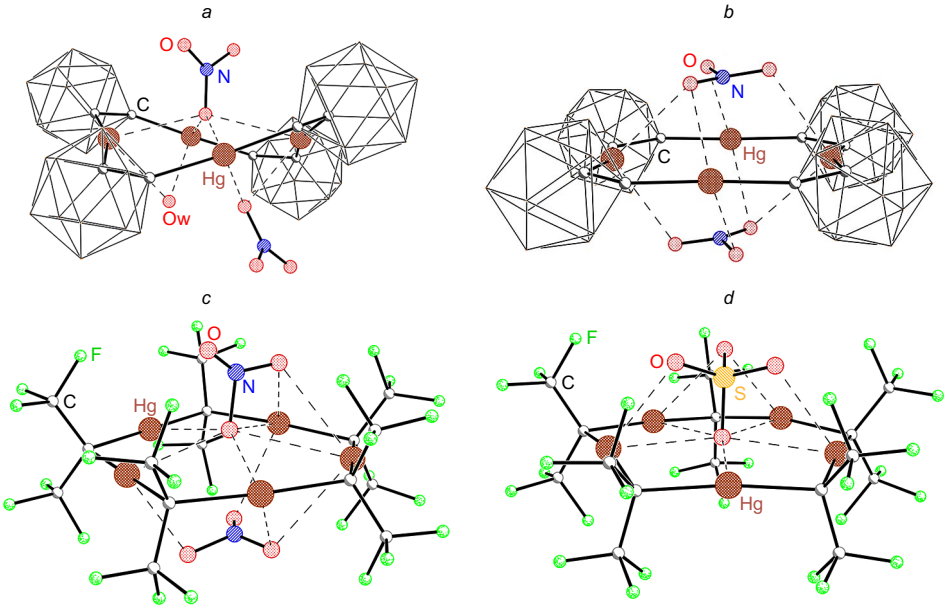


Figure 16. Structures of anionic complexes of four- and five-mercury macrocycles with (*a* – *c*) nitrate and (*d*) sulfate ions. Bipyramidal complexes in structures of compounds (*a*) **44**,[88] (*b*) **45**,[88] and (*c*) **46**[64] and (*d*) pyramidal complex in the structure of compound **47**.[64] Created by the authors based on the data of the aforementioned studies.

(η^1-coordination) correspond to the optimal arrangement of anion and macrocycle with the largest number of Coulomb contacts.

5. Complexes of macrocycle L1 with neutral molecules

Systematic studies of complexing with neutral guest molecules have been performed for only the planar three-mercury macrocycle **L1** (146 structures, according to the CSD). For the rest of the macrocycles, there are only scattered data on the random formation of complexes with polar solvents, in which chemical reactions have been carried out. There are known structures of adducts of macrocycle **L2** with *o*-xylene or acetonitrile;[63] macrocycle **L3** with *o*-xylene, acetonitrile, or acetone;[72] macrocycle **LB1** with acetonitrile,[60,92] acetone, and water;[93] and macrocycle **LB2** with THF and water.[65] In our opinion, the current situation can be explained by several reasons. Due to the planar structure and coordination availability of mercury atoms, the macrocycle **L1** forms a large variety of complexes with guest molecules of different nature, thus providing model compounds for studying the complexing of mercury-containing anticrowns. The macrocycle planar structure facilitates also the formation of stable supramolecular associates, which opens ways to design new crystalline materials. Finally, the relative availability and simplicity of macrocycle synthesis allows many research teams to contribute to this field.

The results of the first structural study of macrocycle **L1** for a crystal solvate with 4-phenylpyridine, which, as the authors noted, does not form shortened intermolecular contacts with the macrocycle, were published in 1981.[94] In the same study, the ability of macrocycle **L1** to form adducts with polar organic molecules was described based on IR and Raman spectroscopy, thermogravimetry, and microanalysis data. However, the structure of these adducts was not determined. The structural variety of the complexes of macrocycle **L1** with neutral molecules having Lewis base properties was demonstrated later in X-ray diffraction studies of its adducts with nitriles, ketones, amides, aldehydes, nitro compounds, aromatic molecules, *etc*. Some results of the first structural analyses were considered in reviews.[28,36] However, many new compounds with macrocycle **L1** have been synthesized in the last decade, and the comparison of the structural data for all investigated classes of neutral guest molecules becomes a relevant task.

5.1. Molecular complexes with neutral Lewis bases

The first molecular complexes of macrocycle **L1** with neutral guest molecules possessing Lewis base properties were obtained for organic nitriles and carbonyl compounds (Fig. 17).[95–100] The interaction of the C=O and C≡N groups with the macrocycle activates molecules in subsequent reactions of nucleophilic addition.[28] The interest in the application of such adducts in organic synthesis and catalysis is still retained.[101–103]

In contrast to the anion complexes of macrocycle **L1**, which are sandwich or multidecker structures, the complexes of this macrocycle with neutral monofunctional Lewis bases are characterized by a pyramidal (1 : 1 composition) or bipyramidal (1 : 2 composition) structure (Table 7).

All complexes contain a common moiety, in which the nucleophilic centre of guest molecule is bound to all mercury atoms of the macrocycle (η^3-coordination). Moreover, an additional guest molecule may be bound to each

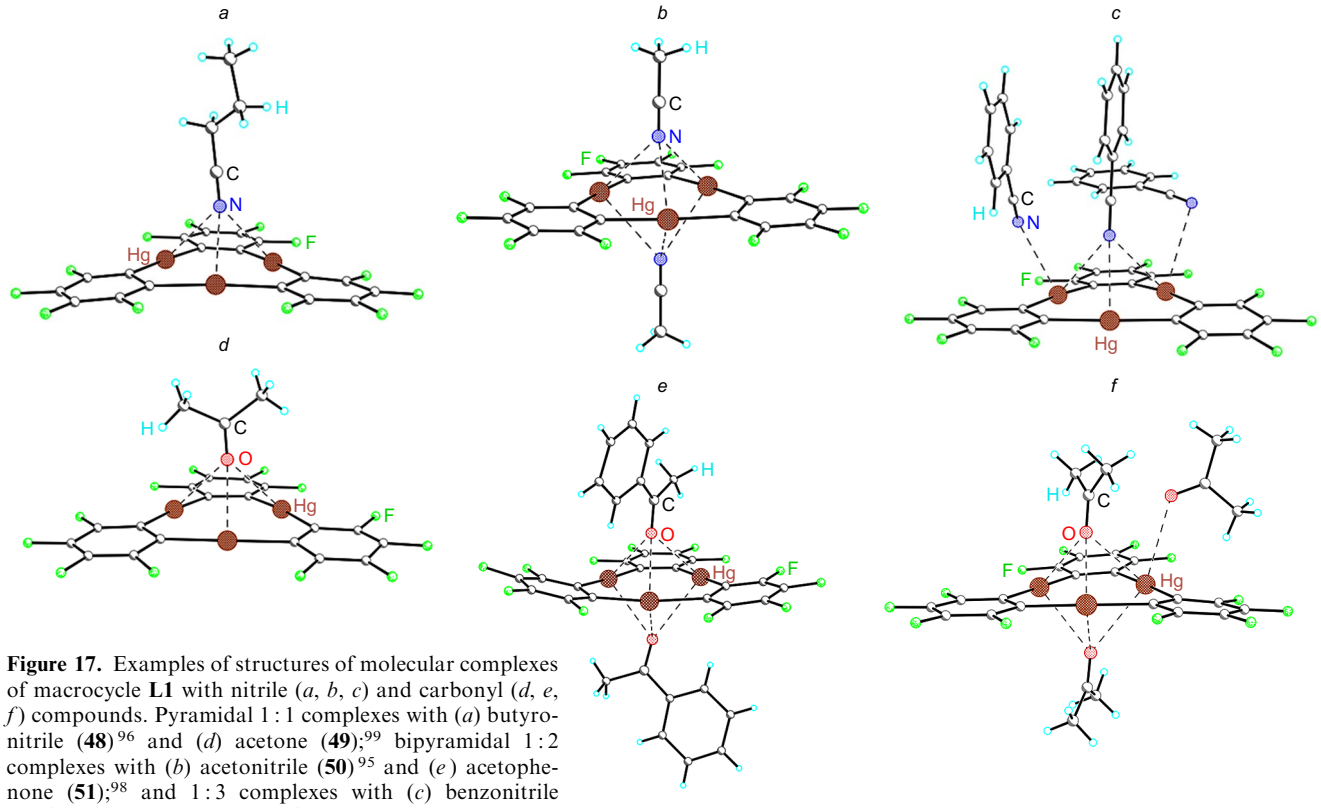
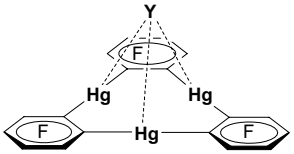
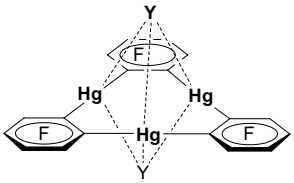
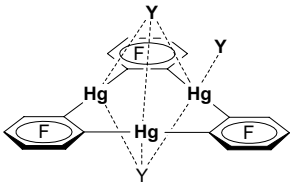
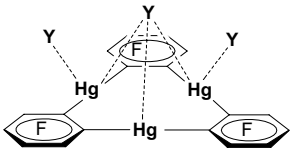


Figure 17. Examples of structures of molecular complexes of macrocycle **L1** with nitrile (*a*, *b*, *c*) and carbonyl (*d*, *e*, *f*) compounds. Pyramidal 1 : 1 complexes with (*a*) butyronitrile (**48**)[96] and (*d*) acetone (**49**);[99] bipyramidal 1 : 2 complexes with (*b*) acetonitrile (**50**)[95] and (*e*) acetophenone (**51**);[98] and 1 : 3 complexes with (*c*) benzonitrile (**52**)[95] and (*f*) acetone (**53**).[98] Created by the authors based on the data of the aforementioned studies.

Table 7. Structure type of the complexes of macrocycle **L1** with neutral monofunctional Lewis bases (Y).

Structure type	Y	Ref.
	CH_2=CHCN	95
	Pr^nCN	96
	MeCHO	98
	Me_2CO	99
	Ph_2CO	98
	$(Me_2NC_6H_4)_2CO$	101
	$(ClC_6H_4)CHO$	102
	FcCHO [a]	103
	MeCN	95
	Me_2NCHO	96
	Me_2NAc	97, 100
	$(Me_2N)_3PO$	97
	PhAc	98
	AcOEt	97
	Me_2SO	97
	Me_2CO	98
	PhCN	95

[a] Fc is ferrocenyl.

mercury atom (η^1-coordination), which leads to 1 : 3 complexes. Crystals of 1 : 2 or 1 : 3 complexes are often decomposed in air (with partial loss of guest molecules) to more thermally stable compounds of the 1 : 1 composition, presumably of pyramidal structure.[95–98]

The interactions between the nucleophilic centre of the guest molecule and the macrocycle mercury atoms are assigned to weak ones, with essentially elongated (in comparison with the sum of covalent radii) Hg–Y distances (Y = N, O). Nevertheless, all complexes contain a pyramidal moiety, having the same structure in different crystal environments, a fact suggesting directionality of cooperative interaction with the macrocycle. The following characteristic features of this interaction are distinguished:[36, 64]

— the Hg–N bond lengths of pyramidal moieties of complexes with nitriles fall in a narrow range of 2.87–2.99 Å; the deviation of the C≡N bond vector from the normal to the macrocycle plane is less than 10°; the nitrile group has a cylindrical symmetry with one lone electron pair of nitrogen being symmetrically bound to each mercury atom of the macrocycle;

— the Hg–O bond lengths in pyramidal moieties of complexes with E=O groups (E = C, S, P) vary in a wide range: from 2.76 to 3.12 Å; the deviation of the E=O bond vector from the normal to the macrocycle plane exceeds 20°; the oxygen atom has two lone electron pairs, a feature impeding symmetric binding to three mercury atoms of the macrocycle;

— the Hg–N or Hg–O bond lengths in pyramidal moieties are independent of the complex stoichiometry; for example, for η^3-coordinated acetone molecules in 1 : 1 complex **49** and in 1 : 3 complex **53**, the Hg–O distances are, respectively, 2.87 Å (Ref. 99) and 2.88 Å (Ref. 98);

— pyramidal moieties exhibit dependence of Hg–O distances on the Lewis basicity (donor ability) of nucleophile; the mean values of distances increase in the series DMSO (2.80 Å) < amides (2.85 Å) < ketones (2.90 Å) in correspondence with the decrease in the donor number of these molecules with respect to $SbCl_5$ in 1,2-dichloroethane (Gutman number [104]): DMSO (29.8 kcal mol^{-1}) > amides (26.6–27.8 kcal mol^{-1}) > ketones (17.0–17.1 kcal mol^{-1});

— binding to the macrocycle does not lead to any significant changes in the structure of the molecules involved in complexing; however, the IR spectra exhibit a significant red shift of the stretching vibration band ν(E=O) relative to the uncoordinated Lewis base; this shift increases with an increase in the nucleophile donor ability.[28]

Pyramidal complexes form stable associates in crystals; these associates are stacking dimers, in which the free sides of macrocycles of the complexes are closely spaced (the interplanar spacings are 3.3–3.4 Å) and intermolecular Hg···Hg and Hg···π contacts are formed (Fig. 18). The existence of mercurophilic interactions in stacking dimers with the Hg–Hg distances ranging from 3.512 to 4.093 Å explains the luminescence properties of macrocycle **L1** and its complex with acetone in the solid state.[53, 99, 105] The Hg–Hg distance in a stacking dimer in structure **48** is 3.372(2) Å;[96] it is the shortest among all known intermolecular Hg···Hg contacts without bridging ligands.

In contrast to monofunctional nitrile or carbonyl guest molecules, bifunctional Lewis bases, when interacting with the macrocycle **L1**, form complexes of sandwich structure or multidecker structures, coordinating simultaneously two macrocycle molecules (Fig. 19). A expressive example is the formation of complex **54** in the reaction with acetylacetone,[106] where the macrocycle **L1** binds selectively the less stable keto tautomer (see Fig. 19 *a*). Sandwich complexes of the 2 : 1 composition with acetylacetone (**54**),[106] *p*-benzoquinone (**55**),[107] maleic anhydride (**56**),[107] and nitroxide NIT-Ph (**57**) (NIT-Ph is 4,4,5,5-tetramethyl-2-phenyl-4,5-dihydro-1*H*-imidazole-1-oxyl 3-oxide) have been structurally characterized,[108] as well as multidecker 1 : 1 structures with malononitrile (**58**),[109] malonic ether (**59**),[109] and NIT-Ph (**60**).[108] The binding of oxygen or nitrogen atoms to

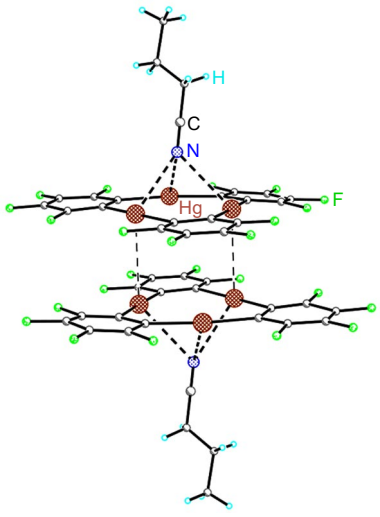


Figure 18. Centrosymmetric stacking dimer in structure **48** of the pyramidal complex with butyronitrile. Dashed lines show the Hg···Hg contacts. Created by the authors based on the data of Ref. 96.

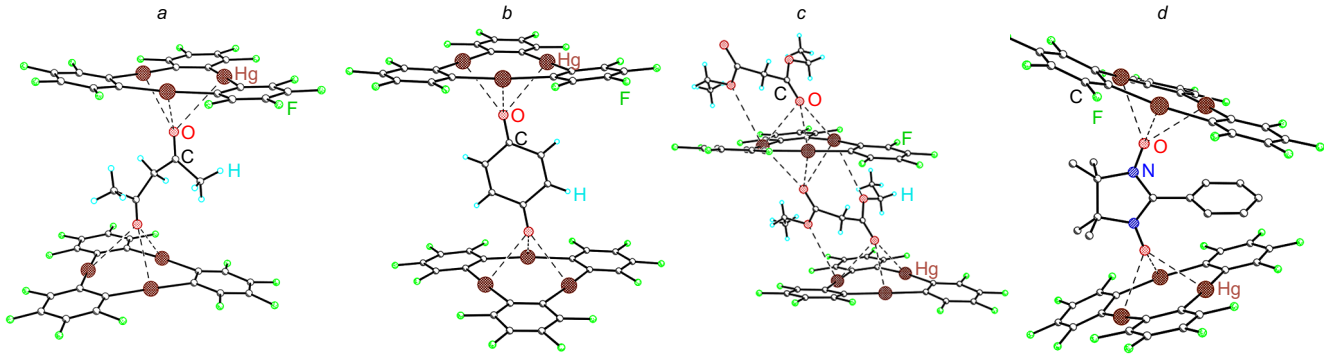


Figure 19. Examples of complexes with bifunctional Lewis bases: (*a*) acetylacetone (**54**),[106] (*b*) *p*-benzoquinone (**55**),[107] (*c*) malonic ether (**59**),[109] and (*d*) nitroxide NIT-Ph (**57**).[108] Created by the authors based on the data of the aforementioned studies.

macrocycles in all complexes is similar to the η^3-coordination in pyramidal moieties of complexes with monofunctional carbonyl or nitrile compounds.

Neutral sandwich complexes form stack packings, in which neighbouring macrocycles are combined into stacking dimers like pyramidal complexes (Fig. 18). In most of sandwich complexes, the macrocycles have a parallel orientation. This structure is stabilized by mutual penetration of stacks shifted by 1/2 or 1/3 of the sandwich height *d* (Fig. 20). The *d* value in all structures is multiple of 3 – 3.5 Å,[64] which corresponds to the conventional distances for stacking contacts between aromatic systems. There is an obvious analogy with stack packings in crystals of anion sandwich complexes (see Fig. 15). The difference is determined by the presence of bulky counter ions, which hinder the formation of close contacts between anion stacks; as a consequence, sandwich moieties acquire a wedge-shaped structure.

The wedge-shaped structure of neutral sandwich compounds is implemented only when the macrocycle **L1** interacts with NIT-Ph (see Fig. 19 *d*). Apparently, this structural feature is determined by the difference in the electronic states of oxygen atom in carbonyl group and nitroxide NO$^{\bullet}$. The N – O bonds in structures **57** and **60** with NIT-Ph, like the C≡N group in complexes with nitriles, are oriented perpendicular to the planes of coordinated macrocycles.[108]

The structure of the complexes of this macrocycle with nitromethane, nitrobenzene, 5-nitroacenaphthene, and 1-nitropyrene has been described.[110] The study of the complexing with nitro compounds was initiated by the data on the high catalytic activity of macrocycle **L1** in phase transfer nitration of aromatic compounds.[111] In addition, the interest in the structure of these complexes is caused by the difference between the coordinating properties of nitro group and the coordinating properties of nitrile

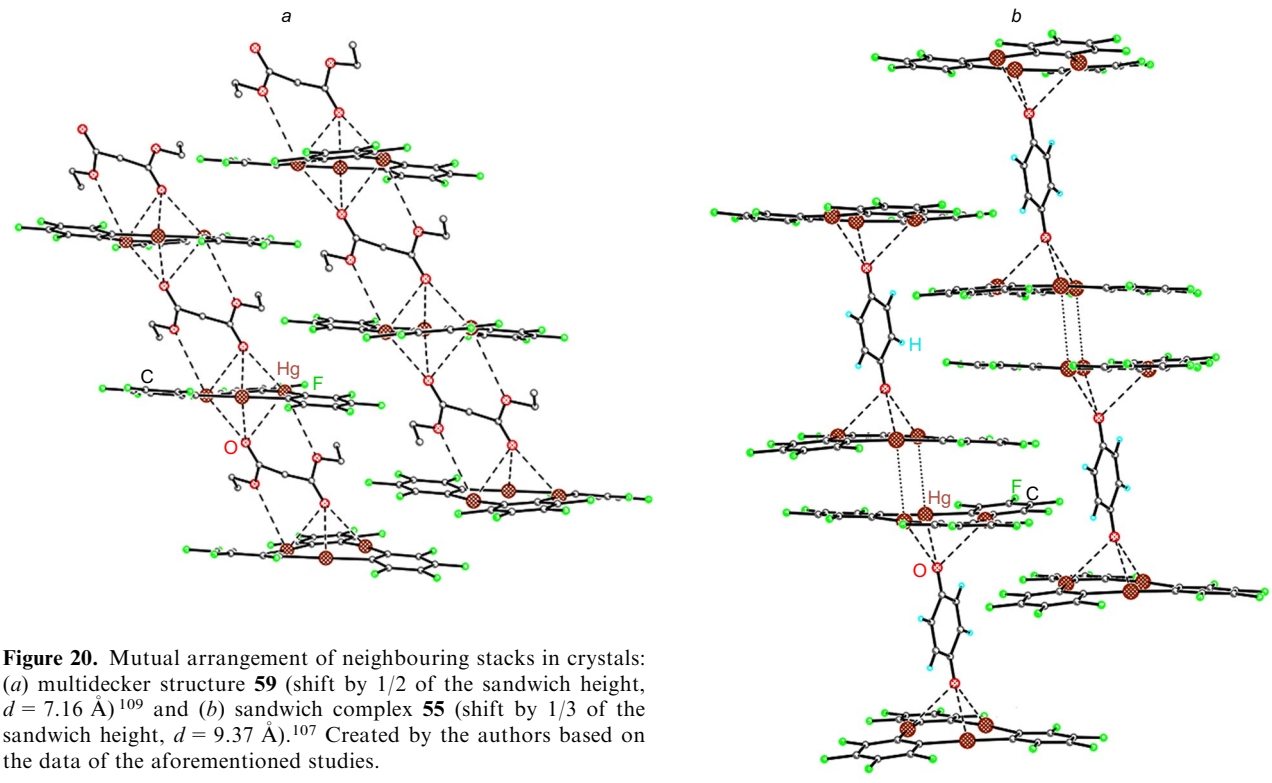


Figure 20. Mutual arrangement of neighbouring stacks in crystals: (*a*) multidecker structure **59** (shift by 1/2 of the sandwich height, d = 7.16 Å)[109] and (*b*) sandwich complex **55** (shift by 1/3 of the sandwich height, d = 9.37 Å).[107] Created by the authors based on the data of the aforementioned studies.

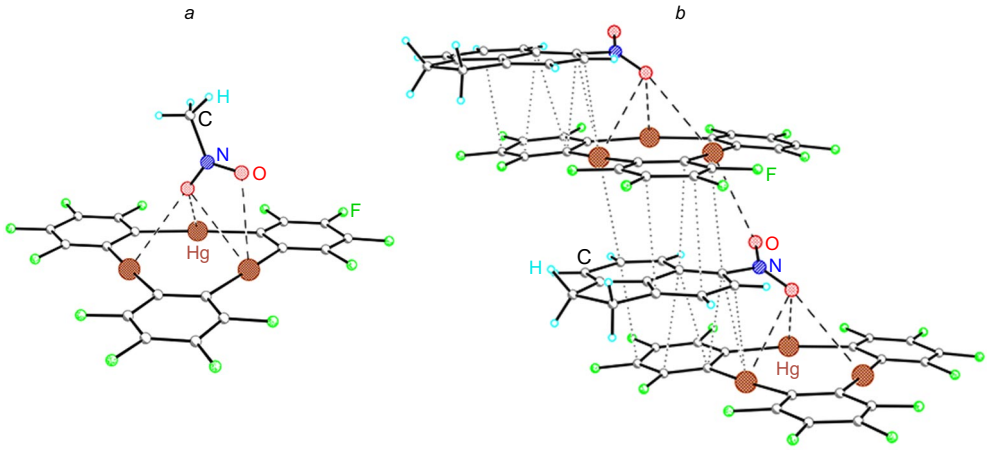


Figure 21. (*a*) Pyramidal complex **61** with nitromethane (the Hg–O distances are 3.03 Å) and (*b*) stack packing of alternating molecules of macrocycle **L1** and 5-nitroacenaphthene in structure **63**. Created by the authors based on the data of Ref. 110.

or carbonyl groups, which contain only one atom with Lewis basicity.

The 1 : 1 complexes with nitromethane (**61**) and nitrobenzene (**62**) have a pyramidal structure, similar to that of the pyramidal complexes with nitriles or carbonyl compounds. Both oxygen atoms of the nitro group are involved in coordination to the macrocycle (Fig. 21 *a*); one of them is bound to three mercury atoms of the macrocycle, while the other is bound to only one mercury atom.[110]

The increase in size of the aromatic system in the guest molecule, as in the complexes with 5-nitroacenaphthene (**63**) and 1-nitropyrene (**64**), diminishes the contribution of the coordination interactions with heteroatoms and, as a consequence, changes the compound structure. The intermolecular stacking Hg···π and π···π interactions (Fig. 21 *b*) with the formation of stack structures become dominant.[110]

5.2. Crystalline adducts with aromatic compounds and other conjugated systems

The ability of macrocycle **L1** to bind aromatic compounds was demonstrated by Professor F.P.Gabbaï *et al.*[36] Adducts are formed due to the secondary interactions of mercury atoms with the electron-saturated π-system of the guest molecule.

The crystal structure of the adduct with benzene (**65**)[112] is built from compact stacks (Fig. 22), which consist of alternating macrocycle and benzene molecules with an interplanar spacing of 3.24 Å. Binding of a benzene molecule is described as the μ_6-η^2:η^2:η^2:η^2:η^2:η^2-coordination with the Hg–$C_{benzene}$ distances equal to 3.408 and 3.457 Å. The large number of weak contacts increases the adduct stability (according to the thermogravimetric data, benzene loss begins 70 °C).[112] In addition, it is suggested that directional interactions are formed due to the donation of electron density from the π-orbitals of benzene C–C bonds to the unoccupied 6p-orbital of mercury atoms [the benzene rotation barrier is estimated to be 52(4) kJ mol^{-1}].[113]

Stack packings are also formed in crystalline adducts of macrocycle **L1** with polycyclic aromatic hydrocarbons: naphthalene, biphenyl, triphenylene,[114] fluorene,[115] pyrene,[116] and phenanthrene.[117] These stacks are formed due to the secondary Hg···π interactions with Hg–C_{arom} interatomic distances of 3.2–3.5 Å and approximately the same interplanar spacings of 3.3 Å.[64] Additional stabilization of guest molecules in stacks occurs due to the stacking interactions of their aromatic moieties with the perfluorophenylene rings of macrocycles.

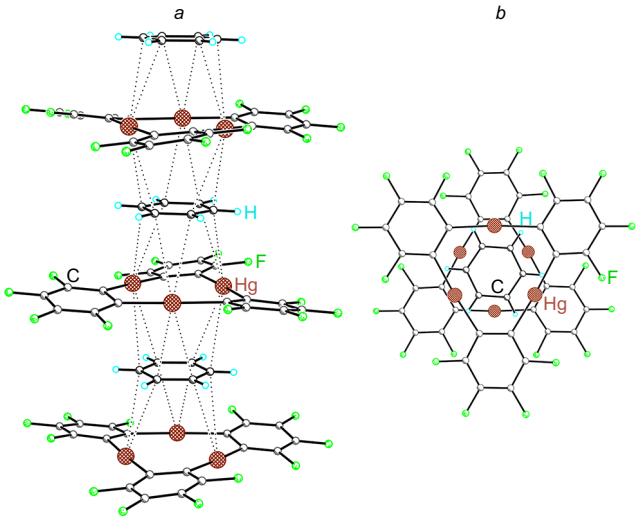


Figure 22. (*a*) Fragment of stack packing in crystal structure **65** of the adduct of macrocycle **L1** with benzene and (*b*) mutual orientation of the macrocycles and guest molecule in a sandwich moiety in structure **65**. Dotted lines are the shortened Hg···$C_{benzene}$ contacts. Created by the authors based on the data of Ref. 112.

The photophysical properties of the adducts of macrocycle **L1** with aromatic molecules were described in detail by Taylor *et al.*[36] For example, adducts with pyrene, naphthalene, and biphenyl exhibit, respectively, red, blue, and green luminescence, which makes them promising for organic light-emitting diode (OLED) technologies.[116]

The structure of adducts with toluene, *o*-xylene, *m*-xylene, *o*-xylene, and mesitylene was studied to trace the influence of steric factors.[118] Stacks of alternating macrocycle and substituted-arene molecules with Hg–C_{arom} distances of 3.2–3.5 Å were found to be formed in all structures. It was noted that aromatic molecules are oriented randomly relative to the macrocycle, which is explained by the weakness of donor–acceptor interactions and significant contribution of less directed electrostatic and dispersion forces.[113,118]

The influence of electron factors on the coordination of aromatic system with macrocycle **L1** was studied by an

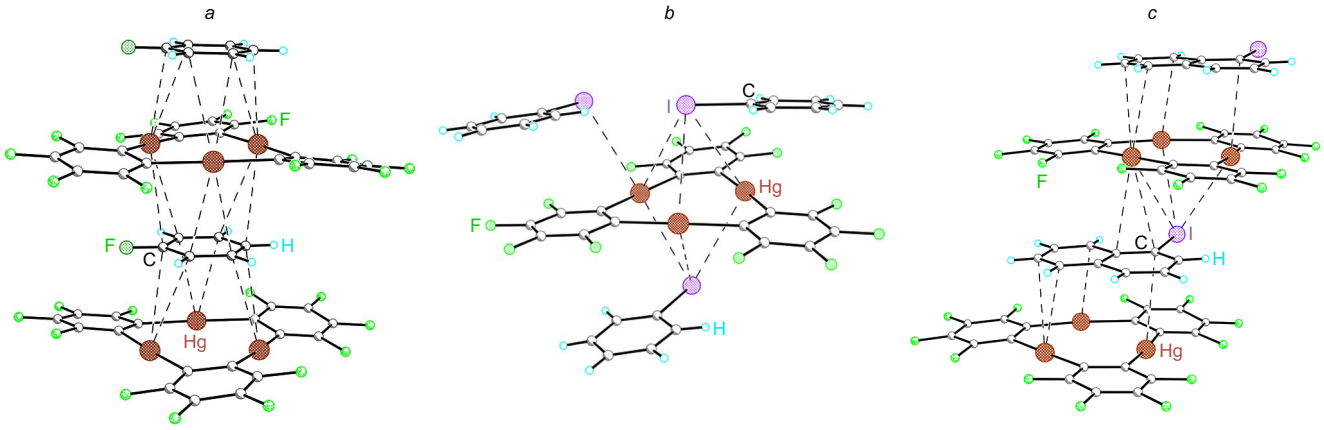


Figure 23. (*a*) Fragment of stack packing in the crystal structure of the adduct of macrocycle **L1** with fluorobenzene,[119] (*b*) 1 : 3 complex with iodobenzene (the coordination is similar to that for 1 : 3 complexes with carbonyl compounds, see Fig. 17*f*),[119] and (*c*) fragment of stack packing in the crystal structure with 1-iodonaphthalene.[120] Created by the authors based on the data of the aforementioned studies.

example of a series of adducts with halobenzenes PhHal (Hal = F, Cl, Br, I).[119] The formation of stacks of alternating macrocycle and arene molecules was observed for only the adduct with fluorobenzene (Fig. 23 *a*), which is isostructural to the benzene adduct **65**. The formation of stack structures is atypical of other halobenzenes, which demonstrate formation of isolated 1 : 2 complexes for chloro- and bromobenzenes or 1 : 3 complex for iodobenzene (Fig. 23 *b*). The interaction of guest halobenzene molecules with the macrocycle occurs mainly with participation of halogen atoms [Hg—Cl = 3.436(3) – 3.709(3), ⟨3.53⟩ Å; Hg—Br = 3.4772(7) – 3.7734(7), ⟨3.58⟩ Å; Hg—I = 3.639(1) – 3.965(1), ⟨3.78⟩ Å], whereas the aromatic rings are located at the periphery of the contact region and involved to a greater extent in the stacking interactions with the perfluorophenylene rings of macrocycles. The Hg—Hal bonds in neutral complexes are significantly elongated (by 0.5 Å on average) in comparison with similar bonds in anionic complexes of mercury-containing anticrowns with halide ions (see Table 5).

In contrast to the interaction with halobenzenes, the interaction of the macrocycle **L1** with 1-halonaphthalenes (Hal = Cl, Br, I)[120] leads to the formation of stack structures, similar to that with naphthalene and other polyaromatic molecules (Fig. 23 *c*). The preferred coordination centre is the aromatic system of bicyclic moiety (the Hg—C_{arom} bond lengths are 3.25 – 3.53 Å). The halogen atom participates in the formation of stack packing only in the structure with 1-iodonaphthalene.[120]

The elongation of the conjugation chain in the guest molecule makes its coordination to the macrocycle stronger and more favourable. In adducts with benzene derivatives (benzonitrile,[95] acetophenone,[98] nitrobenzene,[110] halobenzenes[119]), the main coordination centre is the electron-donating heteroatom. In adducts with polycyclic compounds (5-nitroacenaphthene or nitropyrene,[110] 1-halonaphthalenes[120]), Hg···π interactions form stack structures. It is noteworthy that an increase in the π-system of the guest molecule often leads to spontaneous crystallization, immediately after mixing the components (adducts with triphenylene[114] or pyrene[116]). The adducts with nonplanar polycycles, corannulene and its derivatives, which also have a stack structure in crystals, have been described.[121, 122] Intermolecular interactions in these adducts convert the structure of macrocycle **L1** from planar to bowl-shaped (Fig. 24 *a*). The above facts suggest mainly dispersive interaction with π-conjugated molecules.

The formation of stack structures is observed also for adducts with unsaturated heterocyclic molecules, carbazole[123] and *N*-methylcarbazole.[124] An unexpected result was the formation of the same structure type in complexes with tetrathiafulvalene derivatives[125 – 127] or polycondensed thiophenes[128, 129] (Fig. 24 *b*), for which one would expect coordination to the lone electron pairs of sulfur atoms.

When the macrocycle **L1** interacts with π-acceptors, such as 7,7,8,8-tetracyanoquinodimethane[125] or 1,2,4,5-tetracyanobenzene,[130] coordination occurs to the nitrile groups (the Hg—N distances are 3.01 – 3.34 Å), similar to the η^3-coordination of nitriles in complexes **48**, **50**, and **52**. Under these conditions the π-system of guest molecules is oriented perpendicular to the macrocycle plane and is not involved in binding to the macrocycle (Fig. 24 *c*).

Adducts with acyclic π-systems, such as polyynes, were described[131, 132] (Fig. 24 *d*). The coordination is determined by the interaction of mercury atoms with the polarized π-system of aromatic substituents rather than with the more rigid acetylene groups.

Electrostatic interactions contribute strongly to the stabilization of the adducts of mercury-containing macrocycle **L1** with polar π-systems. This feature was demonstrated by the example of adducts with azulene (**66**) and 6-(*N*,*N*-dimethylamino)pentafulvene (**67**),[132] whose molecules can be presented by resonance forms with charge separation (Scheme 1).

Stack structures **66** and **67** exhibit a general regularity in the arrangement of the five-membered ring in the space between the parallel macrocycle planes, whereas the rest of the guest molecule is located at the periphery (Fig. 25 *a*). The interplanar spacings in the sandwich moiety of structure **67** are 3.17 Å, and the Hg···C contacts are shortened to 3.07(2) Å, a distance much shorter than that in the structures with benzene and other aromatic molecules.

There are published data on the complexing with ferrocene (**68**)[134, 135] and nickelocene.[134] Complexes with metallocenes have an unusual double sandwich structure, in which a metallocene is located between two parallel macrocycles (Fig. 25 *b*). The characteristics of Hg···π-contacts between Cp (cyclopentadienyl) ligands and macrocycles

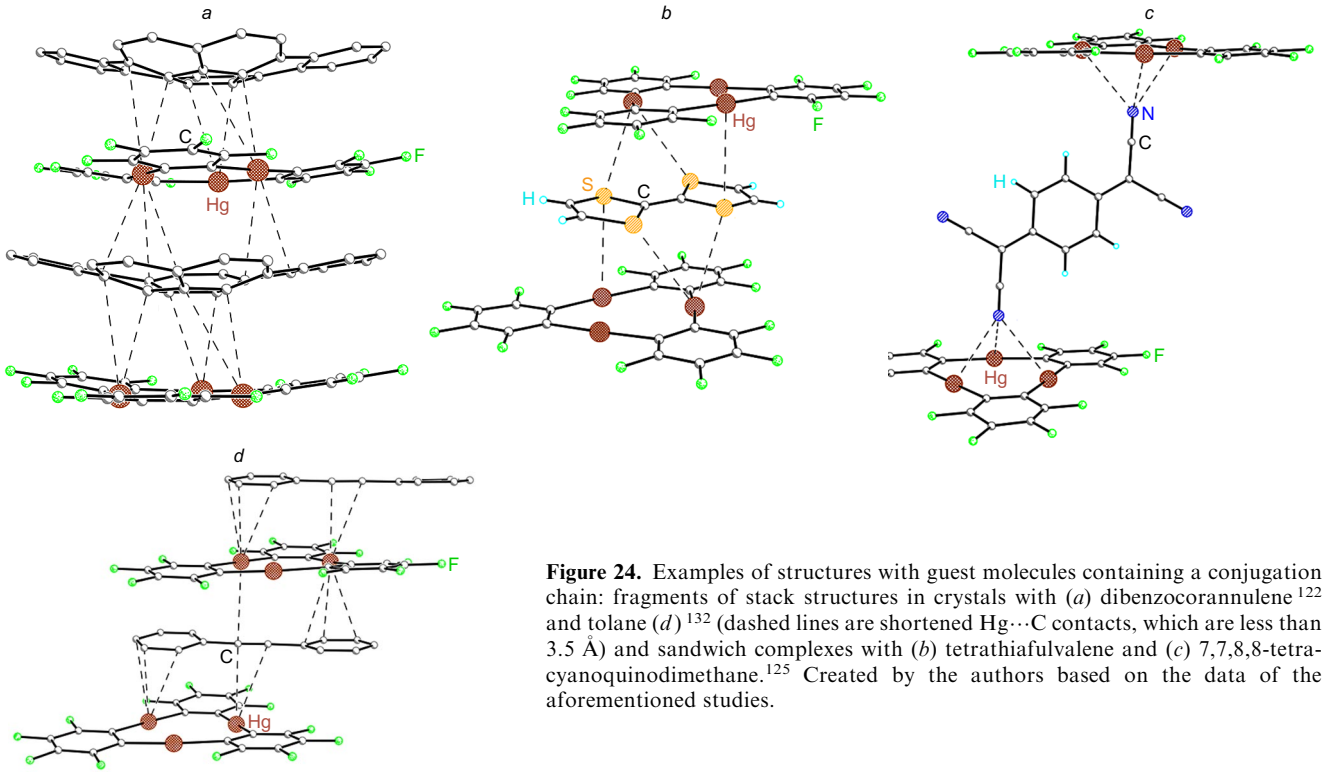
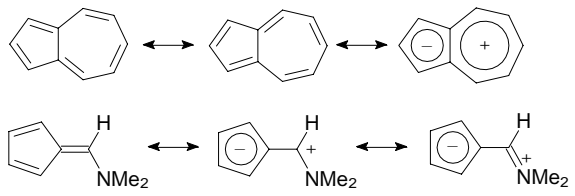


Figure 24. Examples of structures with guest molecules containing a conjugation chain: fragments of stack structures in crystals with (*a*) dibenzocorannulene [122] and tolane (*d*) [132] (dashed lines are shortened Hg···C contacts, which are less than 3.5 Å) and sandwich complexes with (*b*) tetrathiafulvalene and (*c*) 7,7,8,8-tetracyanoquinodimethane.[125] Created by the authors based on the data of the aforementioned studies.

Scheme 1



coincide with those observed in stack structures **66** and **67**. A similar sandwich structure is observed for the complex with paracyclophane,[136] in which benzene rings are bound to macrocycles according to the η^2:η^2:η^2-type [the Hg–C_{arom} distances are 3.110(4)–3.557(4), ⟨3.39⟩ Å], similar to the benzene coordination in structure **65**.

The competition of different electron-saturated moieties for the coordination to macrocycle **L1** during its complexing with heterocyclic ferrocene analogues, pentaphosphaferrocene and pentaarsaferrocene [Cp*Fe(η^5-E_5)] (Cp* is pentamethylcyclopentadienyl, E = P or As) (Fig. 26 *a*,*b*) was studied.[137] The cyclic ligands P_5 or As_5 are isoelectronic analogues of the Cp ligand with a delocalized π-system; each heteroatom has simultaneously a lone electron pair, which forms an alternative way for binding to the macrocycle. The cyclic As_5 ligand of pentaarsaferrocene, as well as Cp in complex **68**, is oriented almost parallel to the macrocycle plane and forms several shortened Hg···As contacts, which indicates participation of the π-electron density of heterocycle in binding with mercury atoms (Fig. 26 *b*). In contrast, in the complex with pentaphosphaferrocene, the lone pair of one out of five phosphorus atoms of the P_5 ligand is involved in binding to the macrocycle (see Fig. 26 *a*) with the formation of a pyramidal structure. In this geometry, the five-membered heterocycle is oriented

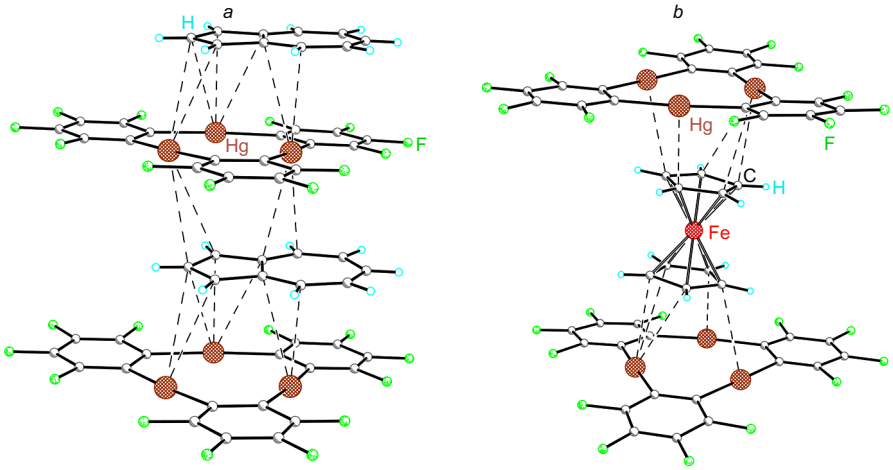


Figure 25. (*a*) Fragment of stack structure **66** with azulene [Hg–$C_{azulene}$ = 3.178(9)–3.584(9) Å] [133] and (*b*) sandwich complex **68** with ferrocene [Hg–C_{Cp} = 3.189(10)–3.561(14) Å].[134,135] Created by the authors based on the data of the aforementioned studies.

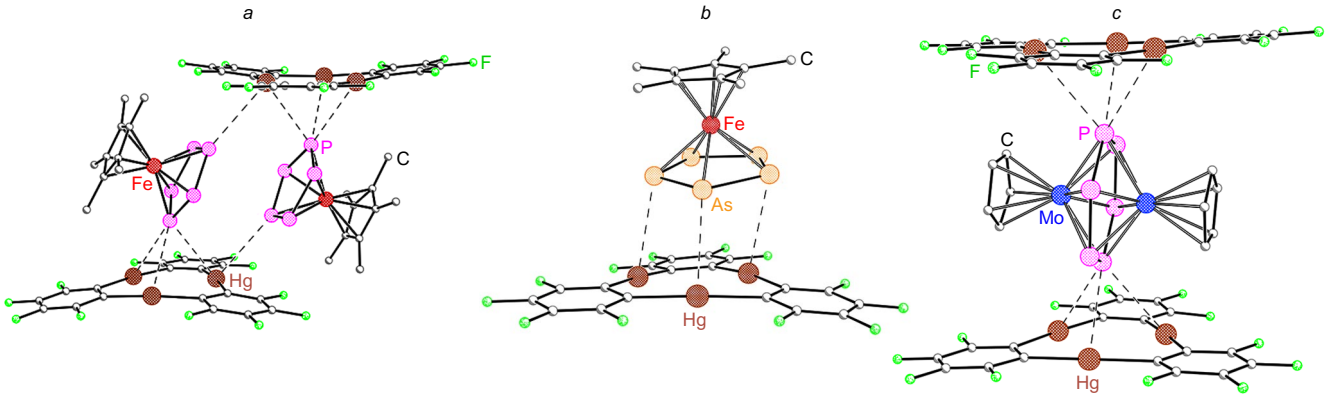


Figure 26. Structure of the adducts of macrocycle **L1** with heterocyclic analogues of metallocenes: (*a*) sandwich dimer of the complex with [Cp*Fe(η^5-P_5)] [distances Hg–P = 3.2878(9)–3.5281(11) Å],[137] (*b*) complex with [Cp*Fe(η^5-As_5)] [distances Hg–As = 3.3014(4)–3.6325(5) Å],[137] and (*c*) sandwich complex with [$(CpMo)_2(\mu$-η^6:η^6-$P_6)$] [mean distance Hg–P = ⟨3.36⟩ Å].[138] Created by the authors based on the data of the aforementioned studies.

almost perpendicular to the macrocycle plane (the dihedral angle is 62°). The preferred coordination of cyclic P_5 ligand *via* the lone pairs of phosphorus atoms is confirmed by the similar structure of three adducts with different sets of steric substituents in the cyclopentadienyl ligand of pentaphosphaferrocene [$Cp^RFe(\eta^5$-$P_5)$], where $Cp^R = C_5H_{5-n}Bu^t_n$, $n = 1-3$.[137]

The structure of the adducts of macrocycle **L1** with a three-decker molybdenum complex [$(CpMo)_2(\mu$-η^6:η^6-$P_6)$] has been described (Fig. 26 *c*); the coordination in these adducts is implemented only to the lone pairs of phosphorus atoms, while Cp ligands are not involved in binding to the macrocycle.[138]

Based on the DFT calculations and analysis of electrostatic potential distribution for a series of adducts with complexes containing E_2 ligands (E = P, As, Sb, Bi), it was concluded that the character of interaction with a mercury-containing macrocycle is mainly electrostatic.[139]

5.3. Complexes with crown ethers and their heteroanalogues

Mercury-containing anticrowns, capable of binding anions, are peculiar antipodes of crown ethers, which exhibit a high affinity to cations. This charge-inverted analogy suggests complexing between crown compounds and anticrowns. Currently the creation of such ditopic ligands is of great interest for studying the biochemical processes of pair transport of various ions through a cell membrane.[26]

Adducts with crown ethers (12-crown-4, 18-crown-6, 15-crown-5, and 1,3,5-trioxane)[140,141] and their heteroanalogues containing sulfur atoms (9-thiacrown-3 and 1,3,5-trithiane)[142] or nitrogen [octaazapentacyclooctacosane, 1,4,8,11-tetraazacyclotetradecane (cyclam) and *N*,*N*,*N*-trimethyl-1,3,5-triazacyclohexane] have been obtained for the macrocycle **L1**.[143] Symmetric complexes of cellular structure are formed with six-membered heterocycles: 1,3,5-trioxane (Hg–O = 2.87 Å[140]), 1,3,5-trithiane (Hg–S = 3.20 Å[142]), and *N*,*N*,*N*-trimethyl-1,3,5-triazacyclohexane (Hg–N = 2.91 Å[143]) (Fig. 27 *a*). Adducts with

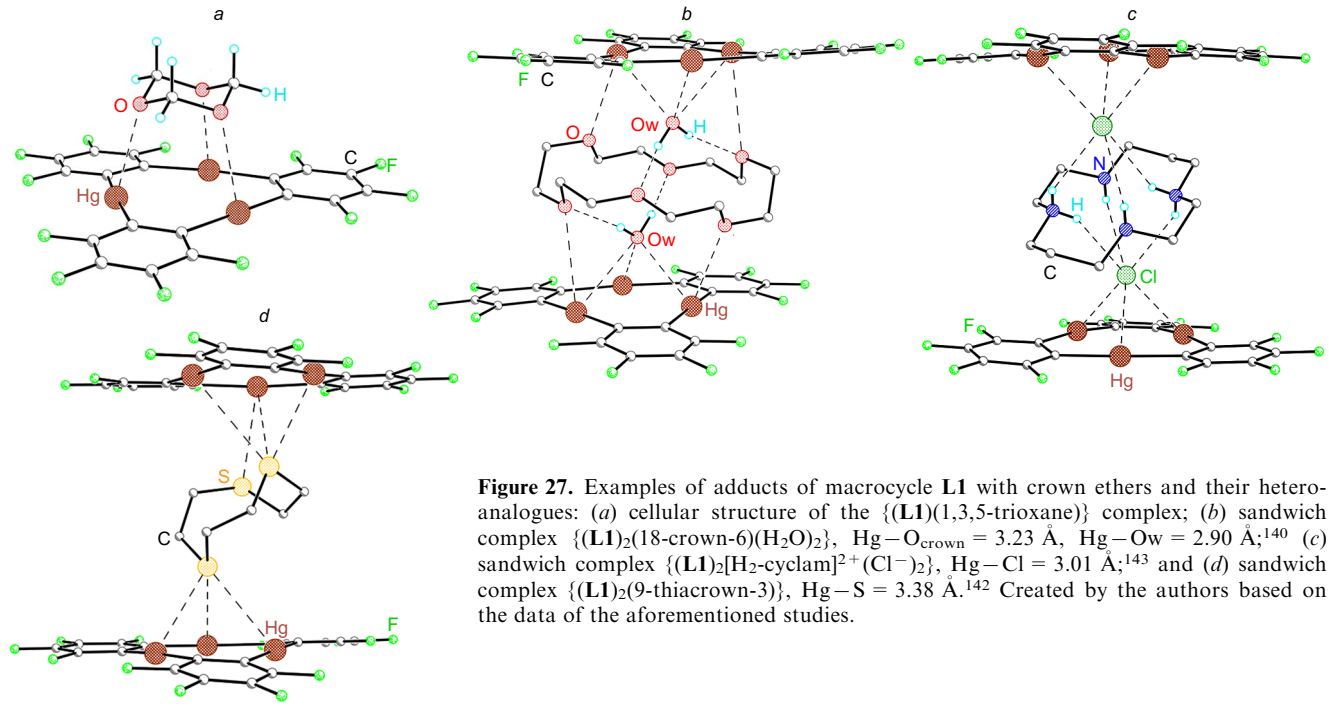


Figure 27. Examples of adducts of macrocycle **L1** with crown ethers and their heteroanalogues: (*a*) cellular structure of the {(**L1**)(1,3,5-trioxane)} complex; (*b*) sandwich complex {$(\mathbf{L1})_2$(18-crown-6)$(H_2O)_2$}, Hg–O_{crown} = 3.23 Å, Hg–Ow = 2.90 Å;[140] (*c*) sandwich complex {$(\mathbf{L1})_2[H_2$-cyclam$]^{2+}(Cl^-)_2$}, Hg–Cl = 3.01 Å;[143] and (*d*) sandwich complex {$(\mathbf{L1})_2$(9-thiacrown-3)}, Hg–S = 3.38 Å.[142] Created by the authors based on the data of the aforementioned studies.

oxygen- or nitrogen-containing macrocyclic molecules have multicomponent compositions, where the interaction with a mercury-containing macrocycle is implemented either with participation of solvate water molecules (characteristic of crown ethers)[140] or a chloride ion formed as a result of cyclam molecule protonation in chlorine-containing solvents[143] (Fig. 27 *b*,*c*). Direct contacts between macrocyclic molecules are rare. In contrast, reactions with sulfur-containing molecules give rise to complexes only due to the interaction between crown and anticrown macrocyclic molecules (Fig. 27 *d*).[142] This difference in the heterocycle coordination is explained by the favourability of the interaction of easily polarizable mercury atoms with sulfur atoms (soft base) in comparison with rigid oxygen or nitrogen atoms. NMR data also indicate the preference of complexing of macrocycle **L1** with sulfur-containing molecules.[142]

5.4. Macrocycle L1 in coordinating solvents

The macrocycle **L1** is virtually insoluble in noncoordinating and nonpolar solvents. Therefore, polar solvents (THF, alcohol, CH_2Cl_2, *etc*.) are used to perform spectroscopic measurements and carry out reactions with guest molecules. However, the solvent molecule competes with the guest molecule, coordinating macrocyclic mercury atoms, which leads to dissociation of host – guest complexes with relatively weak Lewis bases, such as crown ethers[140,142] and nitrile,[95,96] carbonyl,[97,107] or nitro compounds.[110]

Structural studies of the adducts of macrocycle **L1** with the most popular solvents yielded some information about the behaviour of mercury-containing anticrowns in solutions. Complexes with acetone,[98,99] acetonitrile,[95] THF,[144] ethanol,[144] and methylene chloride[137] were characterized. Different crystallization conditions lead to the formation of different structures, in which one macrocycle assembles from one to four solvent molecules around itself. Similar examples were described for adducts with acetone[98,99] (1 : 1 and 1 : 3 complexes) or dimethyl sulfide[145] (1 : 1 and 1 : 4 complexes). The product of crystallization from THF is a cocrystal of 1 : 2, 1 : 3, and 1 : 4 complexes in structure **69** (Fig. 28). The example of this cocrystal shows most clearly that complexes of mercury-containing macrocycle with different numbers of coordinated solvent molecules are simultaneously present in solution. One would suggest that the macrocyclic mercury atoms will be shielded to a greater extent with an increase in the solvent coordinating ability. The coordinative saturation of mercury atoms with solvent molecules should hinder their coordination with guest molecules. The revealed specific features of the solvation of mercury-containing macrocycles must be taken into account when obtaining new molecular host – guest complexes in a medium of coordinating solvents.[64]

5.5. Models of binding macrocycle L1 to neutral Lewis bases

The favourability of the η^3-coordination of electron-saturated moiety of guest molecule is confirmed by *ab initio* calculations (DFT method) of the electronic structure of mercury-containing macrocycle **L1**.[36,108,146] The calculations show that the highest occupied molecular orbital (HOMO) is localized mainly on perfluorophenylene rings, whereas the main contribution to the lowest unoccupied molecular orbital (LUMO) is from the 6p orbital of mercury atoms (44%).[108] The central part of the macrocycle, where the Lewis acid properties are most pronounced, determines the direction along which the guest nucleophilic molecule interacts with the macrocycle (Fig. 29). The calculated energy difference for the frontier orbitals is 3.36 eV;[108] *i.e*., the LUMO of the macrocycle is high on the energy scale and thus cannot be efficiently overlapped with the guest-molecule donor orbitals. Therefore, it was suggested[36,108] that the binding in complexes of mercury-containing macrocycle **L1** with neutral Lewis bases is determined to a greater extent by electrostatic rather than covalent (donor – acceptor) interactions. This property is clearly demonstrated by the electrostatic potential distribution, where the positive potential is localized in the central part of the macrocycle and the negative potential is localized at the periphery of fluorinated macrocycle (see Fig. 29).[146]

Depending on the nature of the guest nucleophilic centre, one can observe systematic differences in the structural characteristics of the pyramidal moieties formed in the case of η^3-coordination; for example, in complexes with carbonyl and nitrile compounds (see Section 5.1). The same structural features of pyramidal moieties were observed in 1 : 1 complexes of macrocycle **L1** with EtOH (**70**), THF (**71**),[144] and Me_2S (**72**)[145] (Fig. 30). The plane of oxygen atoms in structures **70** and **71**, which is set by two substituents, is oriented perpendicular to the macrocycle plane, and the Hg – O distances are nonequivalent (Table 8). The dimethyl sulfide molecule, bound symmetrically to all mercury atoms, is located in the bisectral plane of the wedge-shaped moiety of multidecker structure **72** (see Table 8). Based on the structural data, the binding of dimethyl sulfide to macrocycle **L1** is described[145] as a four-centre two-electron interaction due to the overlap of the sulfur unshared electron pair, directed towards the macrocycle centre, with three unoccupied 6p orbitals of mercury atoms (Fig. 31 *a*). Similar considerations can be used to describe

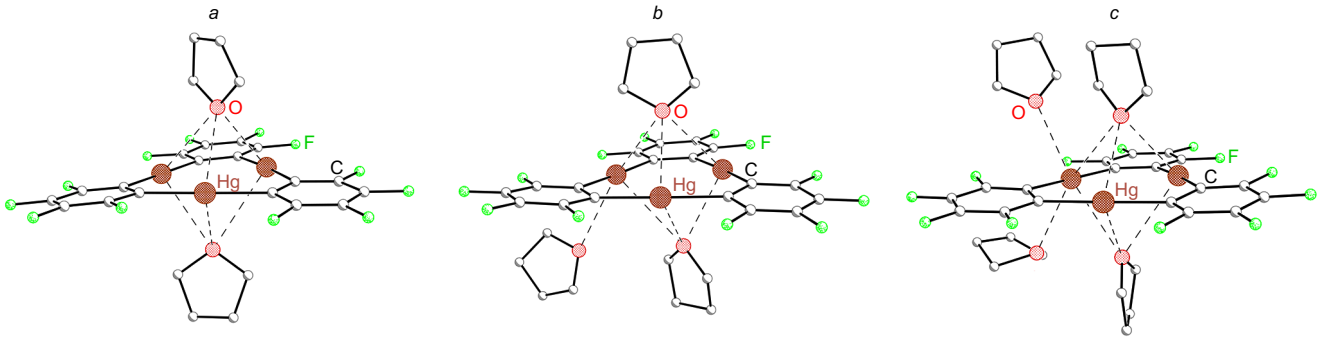


Figure 28. Complexes of macrocycle **L1** with THF of the (*a*) 1 : 2, (*b*) 1 : 3, and (*c*) 1 : 4 compositions in the structure of co-crystallizate **69**. Created by the authors based on the data of Ref. 144.

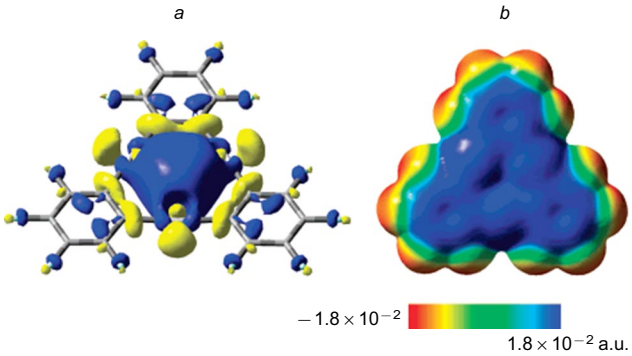


Figure 29. (*a*) Lowest unoccupied molecular orbital and (*b*) electrostatic potential surface in the macrocycle **L1** according to the DFT data.[36] Presented with kind permission of the ACS Publications.

the binding of the oxygen atom of ether or carbonyl groups or the nitrogen atom of nitrile groups with the macrocycle **L1** (Figs. 31 *b*,*c*).[64]

These simple geometric representations are confirmed by the quantumchemical calculations of crystal structures **71** and **72** (PBE functional, plane-wave basis set).[144] An analysis of the electron density function $\rho(r)$ showed that one lone pair of O(1) is located on the Hg(1)–O(1) line (Fig. 32 *a*), while the other is directed towards the centre of the opposing C–C bond of the macrocycle (Fig. 32 *b*). The critical points CP(3, –1), corresponding to interatomic interactions,[147] were found for three Hg–O bonds of the guest molecule with the macrocycle. An estimation of the Hg···O interaction energy from the calculation data confirms their nonequivalence [the Hg(1)–O(1) coordination bond is energetically more favourable (by a factor of about 3) than the two other Hg–O bonds] and yields total values

Table 8. Hg–Y bond lengths (Å) in complexes **70**, **71**,[144] and **72**.[145]

Bond	Complex **70** (Y = O)	Complex **71** (Y = O)	Complex **72** (Y = S)
Hg(1)–Y	2.907(3)	2.853(3)	3.571(3)
Hg(2)–Y	3.145(3)	3.251(3)	3.543(7)
Hg(3)–Y	3.134(3)	3.229(3)	3.576(7)

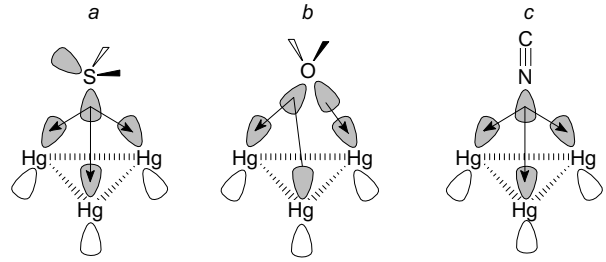


Figure 31. Multicentre interaction of (*a*, *c*) one or (*b*) two lone pairs of heteroatom with the macrocycle **L1**.[64]

of 7.1 and 7.6 kcal mol^{-1} for complexes **71** and **72**, respectively.[144] Thus, binding occurs with participation of all mercury atoms of the macrocycle, but with significantly different lengths and energy characteristics of coordination Hg–O bonds. The directionality and nonequivalence of these interactions are determined by the orientation of the lone pairs of the oxygen atom.[144]

Based on the calculated characteristics of the function $\rho(r)$ at CP(3, –1), the Hg–O bonds were described as interactions of closed shells, and it was concluded that these interactions have preferred electrostatic character.[144] The same conclusion about the mainly electrostatic and (or) dispersion character of interaction of three-mercury macrocycle with neutral guest molecules was drawn proceeding from analysis of the calculated function $\rho(r)$ in adducts with pentaphosphaferrocene and pentaarsaferrocene [Cp*Fe(η^5-E$_5$)], where E = P or As;[137] with molybdenum complexes containing E$_2$ ligands (E = P, As, Sb, Bi);[139] and with the Ni(salen) complex.[148]

Along with the interactions with the guest molecule, the interactions between the host molecules also play an important role in the formation of the crystal structure of complexes of macrocycle **L1**. A calculation of the energy of pair intermolecular interactions in polymorphs of macrocycle **L1** showed that the most stable supramolecular association of macrocycles corresponds to the stacking dimers in the stack packings stabilized by the Hg···π and π···π interactions.[57] The following two types are selected among the complexes of macrocycle **L1** with neutral guest molecules:

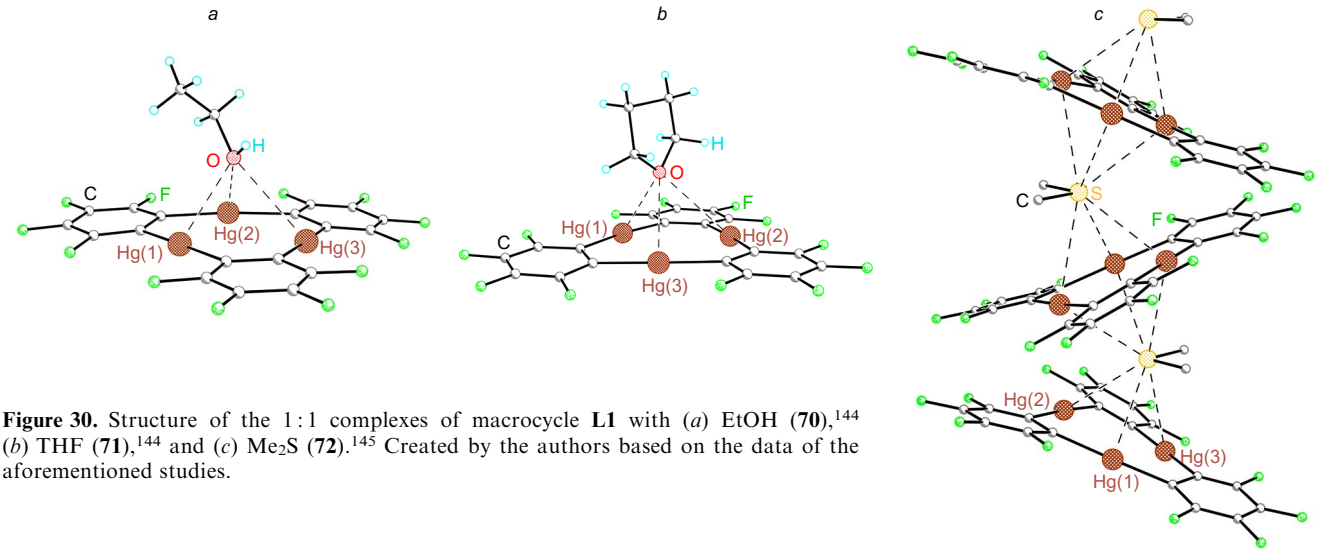


Figure 30. Structure of the 1 : 1 complexes of macrocycle **L1** with (*a*) EtOH (**70**),[144] (*b*) THF (**71**),[144] and (*c*) Me$_2$S (**72**).[145] Created by the authors based on the data of the aforementioned studies.

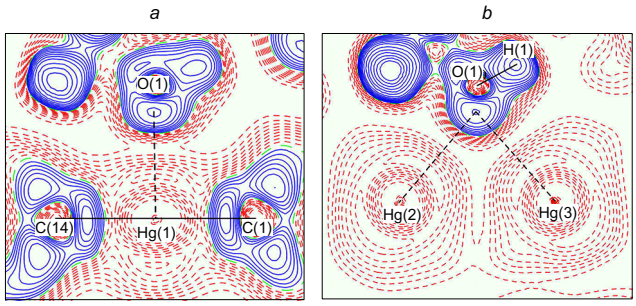


Figure 32. Electron localization function (ELF) cross sections in structure **71** in the (*a*) O(1)–Hg(1)–C(1) and (*b*) O(1)–Hg(2)–Hg(3) planes. The valence electron concentration ranges (ELF > 0.5) are shown by solid blue lines; the isoline step is 0.05.[144] Presented with kind permission of the ACS Publications.

— complexes with Lewis bases, in which binding occurs between electron-deficient mercury atoms of the macrocycle and the lone pair of the electron-donating heteroatom of the guest molecule;

— adducts with unsaturated molecules, containing an open or closed conjugation chain (arenes, polyarenes, polyynes, corannulenes, *etc.*), in which binding is due to the Hg···π and π···π interactions.

The first-type compounds are discrete pyramidal, bipyramidal, or sandwich complexes, whose association in crystals is determined by the ability of macrocycles to form stacking dimers. Crystals of second-type compounds are most often constructed from two-component stacks of alternating macrocycle and guest molecules, similar to the stack packings in polymorphic structures of macrocycle **L1**.[57] The general regularities of the formation of crystal structure of macrocycle **L1** with diverse guest molecules are determined by the similarity of the energetic and geometric characteristics of intermolecular macrocycle···guest and macrocycle···macrocycle interactions.[57] For example, the ability of macrocycle **L1** to structure amorphous mixtures due to the directionality of intermolecular interactions has successfully been used to design components of polymer solar cells.[149]

6. Conclusion

In the recent years, an increasing number of publications have been devoted to the synthesis of metallomacrocyclic compounds and study of their properties.[23, 24, 150, 151] The interest in these compounds is determined by their diverse application potential; in particular, an important issue is the formation of systems for binding and recognizing anions. Guest-molecule binding is due to intermolecular nonvalent interactions. A detailed description of nonvalent interactions, their classification, and the role in the engineering of smart materials and devices can be found in exhaustive review.[152] An analysis of the intermolecular interactions by modern calculation methods[153] can be performed for only the compounds for which the crystal structure was experimentally determined. There is no much progress in the prediction of complex multicomponent structures;[154, 155] therefore, the crystallochemical analysis of existing structures and identification of structural regularities in series of related compounds remain important for their crystal and molecular design.

The regularities of the molecular and crystal structures of complexes of mercury-containing anticrowns with anions and neutral molecules, presented in this review, give grounds to formulate a number of general statements. The following types of stable supramolecular architectures of complexes can be selected: sandwich, pyramid, bipyramid, or guest in the macrocycle cavity (for example, in the complex of **LB2** macrocycle with a fluoride ion). The preference of a particular supramolecular architecture is determined by the macrocycle structure (the presence of steric substituents, conformational rigidity, internal-cavity size) and the number of mercury atoms in it. The cooperative interaction of the nucleophilic centre of the guest with all metal atoms of the macrocyclic host has a pronounced directionality to the macrocycle centre and determines the general structure of the complex.

The good prospects of anticrowns in various applications (such as phase-transfer catalysis and ion-selective applications), as well as the possibility of forming molecular materials with photophysical or magnetic properties, determine the demand for them and initiate the search for new types of macrocyclic hosts. An important step in this direction has been made in the last years; it concerns the synthesis of host–guest complexes of mercury-containing macrocycles **L2** and **L3**. The spatial structure of macrocycles determines their selectivity in binding guest molecules, which indicates their good prospects for various anion-selective applications. Another interesting direction is the search for new macrocyclic hosts, including other metal ions with Lewis acidic properties. For example, a close analogy with the properties of macrocycle **L1** was found for cyclic pyrazolates of Group 11 metals.[156–161]

We believe that the design regularities of supramolecular complexes of mercury-containing macrocycles, described in this review, are general for other macrocyclic Lewis acids and will be useful for further development of the coordination chemistry of anticrowns.

The review was prepared with support of the Russian Foundation for Basic Research (Project No. 19-13-50397), the review was also supported by the Ministry of Science and Higher Education of the Russian Federation as part of the State Assignment of the Kurnakov Institute of General and Inorganic Chemistry of the Russian Academy of Sciences and performed using the equipment of the JRC PMR IGIC RAS on providing access to CSD and electronic libraries.

7. List of acronyms and designations

Cp — cyclopentadienyl,
Cp* — pentamethylcyclopentadienyl,
DFT — density functional theory,
Fc — ferrocenyl,
NIT-Ph — 4,4,5,5-tetramethyl-2-phenyl-4,5-dihydro-1*H*-imidazole-1-oxyl 3-oxide,
OLED — organic light-emitting diode,
PPN — bis(triphenylphosphine)iminium,
r_{cov} — covalent radius,
R_{vdw} — van der Waals radius,
$\rho(r)$ — electron density function,
solv — solvent molecule in crystal solvate.

References

1. J.-M.Lehn. *Angew. Chem., Int. Ed. Engl.*, **27**, 89 (1988)
2. Z.Liu, S.K.M.Nalluri, J.F.Stoddart. *Chem. Soc. Rev.*, **46**, 2459 (2017)
3. Q.He, G.I.Vargas-Zuniga, S.H.Kim, S.K.Kim, J.L.Sessler. *Chem. Rev.*, **119**, 9753 (2019)
4. I.A.Abdulaeva, K.P.Birin, A.Bessmertnykh-Lemeune, A.Yu.Tsivadze, Yu.G.Gorbunova. *Coord. Chem. Rev.*, **407**, 213108 (2020)
5. A.D.Zubenko, O.A.Fedorova. *Russ. Chem. Rev.*, **89**, 750 (2020)
6. C.J.Pedersen. *J. Am. Chem. Soc.*, **89**, 7017 (1967)
7. B.Dietrich, J.-M.Lehn, J.-P.Sauvage. *Tetrahedron Lett.*, **10**, 2889 (1969)
8. H.E.Simmonds, C.H.Park. *J. Am. Chem. Soc.*, **90**, 2431 (1968)
9. D.E.Kaufmann, A.Otten. *Angew. Chem., Int. Ed. Engl.*, **33**, 1832 (1994)
10. J.W.Steed, J.L.Atwood. *Supramolecular Chemistry*. (Wiley, 2000)
11. J.L.Sessler, P.A.Gale, Won-Seob Cho. *Anion Receptor Chemistry*. (Cambridge, UK, 2006)
12. P.A.Gale. *Chem. Soc. Rev.*, **39**, 3746 (2010)
13. N.Busschaert, C.Caltagirone, W.V.Rossom, P.A.Gale. *Chem. Rev.*, **115**, 8038 (2015)
14. M.Wenzel, J.J. Weigand. *J. Incl. Phenom. Macrocycl. Chem.*, **89**, 247 (2017)
15. P.Molina, F.Zapata, A.Caballero. *Chem. Rev.*, **117**, 9907 (2017)
16. L.Chen, S.N.Berry, X.Wu, E.N.W.Howe, P.A.Gale. *Chem.*, **6**, 61 (2020)
17. X.Yang, C.B.Knobler, M.F.Hawthorne. *Angew. Chem., Int. Ed. Engl.*, **30**, 1507 (1991)
18. M.Newcomb, J.H.Horner, M.T.Blanda, P.J.Squattrito. *J. Am. Chem. Soc.*, **111**, 6294 (1989)
19. M.Schulte, M.Schurmann, K.Jurkschat. *Chem. – Eur. J.*, **7**, 347 (2001)
20. M.E.Jung, H.Xia. *Tetrahedron Lett.*, **29**, 297 (1988)
21. J.D.Wuest. *Acc. Chem. Res.*, **32**, 81 (1999)
22. G.Mezei, C.M.Zaleski, V.L.Pecoraro. *Chem. Rev.*, **107**, 4933 (2007)
23. E.Zangrando, M.Casanova, E.Alessio. *Chem. Rev.*, **108**, 4979 (2008)
24. P.Thanasekaran, C.-H. Lee, K.-L. Lu. *Coord. Chem. Rev.*, **280**, 96 (2014)
25. I.Haiduc, F.T.Edelmann. *Supramolecular Organometallic Chemistry*. (New York: Wiley-VCH, 1999)
26. J.W.Steed, D.R.Turner, K.J.Wallace. *Core Concepts in Supramolecular Chemistry and Nanochemistry*. (New York: Wiley, 2007)
27. I.B.Sivaev, M.Yu.Stogniy. *Russ. Chem. Bull., Int. Ed.*, **68**, 217 (2019)
28. V.B.Shur, I.A.Tikhonova. *Russ. Chem. Bull., Int. Ed.*, **52**, 2539 (2003)
29. V.B.Shur, I.A.Tikhonova. In *Encyclopedia of Supramolecular Chemistry*. (Eds J.L.Atwood, J.W.Steed). (New York: Marcel Dekker, 2004). P. 68
30. C.R.Groom, F.H.Allen. *Angew. Chem., Int. Ed.*, **53**, 662 (2014)
31. M.F.Hawthorne, X.Yang, Z.Zheng. *Pure Appl. Chem.*, **66**, 245 (1994)
32. X.Yang, C.B.Knobler, Z.Zheng, M.F.Hawthorne. *J. Am. Chem. Soc.*, **116**, 7142 (1994)
33. M.F.Hawthorne, Z.Zheng. *Acc. Chem. Res.*, **30**, 267 (1997)
34. I.H.A.Badr, R.D.Johnson, M.Diaz, M.F.Hawthorne, L.G.Bachas. *Anal. Chem.*, **72**, 4249 (2000)
35. T.J.Wedge, M.F.Hawthorne. *Coord. Chem. Rev.*, **240**, 111 (2003)
36. T.J.Taylor, C.N.Burress, F.P.Gabbaï. *Organometallics*, **26**, 5252 (2007)
37. D.Grdenić. *Quart. Rev. Chem. Soc.*, **19**, 303 (1965)
38. L.G.Kuz'mina, Yu.T.Struchkov. *Croat. Chem. Acta*, **57**, 701 (1984)
39. L.G.Kuz'mina. *Russ. J. Coord. Chem.*, **25**, 599 (1999)
40. J.S.Casas, M.S.Garcia-Tasende, J.Sordo. *Coord. Chem. Rev.*, **193 – 195**, 283 (1999)
41. F.P.Gabbaï, C.N.Burress, M.-A.Melaimi, T.J.Taylor. In *Comprehensive Organometallic Chemistry III*. Vol. 2. (Eds R.H.Crabtree, D.M.P.Mingos). (New York: Elsevier, 2007). P. 419
42. M.Melník. *Cent. Eur. J. Chem.*, **8**, 469 (2010)
43. B.Cordero, V.Gómez, A.E.Platero-Prats, M.Revés, J.Echeverría, E.Cremades, F.Barragán, S.Alvarez. *Dalton Trans.*, 2832 (2008)
44. A.Bondi. *J. Phys. Chem.*, **68**, 441 (1964)
45. A.J.Canty, G.B.Deacon. *Inorg. Chim. Acta*, **45**, L225 (1980)
46. S.S.Batsanov. *Inorg. Mater.*, **37**, 871 (2001)
47. P.Pyykkoö, M.Straka. *Phys. Chem. Chem. Phys.*, **2**, 2489 (2000)
48. H.Schmidbaur, A.Schier. *Organometallics*, **34**, 2048 (2015)
49. V.B.Shur, I.A.Tikhonova, A.I.Yanovsky, Yu.T.Struchkov, P.V.Petrovskii, S.Yu.Panov, G.G.Furina, M.E.Vol'pin. *Dokl. Akad. Nauk SSSR*, **321**, 1002 (1991)
50. V.B.Shur, I.A.Tikhonova, A.I.Yanovsky, Yu.T.Struchkov, P.V.Petrovskii, S.Yu.Panov, G.G.Furin, M.E.Vol'pin. *Bull. Acad. Sci. USSR, Div. Chem. Sci. (Engl. Transl.)*, **40**, 1305 (1991)
51. V.B.Shur, I.A.Tikhonova, A.I.Yanovsky, Yu.T.Struchkov, P.V.Petrovskii, S.Yu.Panov, G.G.Furin, M.E.Vol'pin. *J. Organomet. Chem.*, **418**, C29 (1991)
52. R.D.Shannon, C.T.Prewitt. *Acta Crystallogr., Sect. B*, **25**, 925 (1969)
53. M.R.Haneline, M.Tsunoda, F.P.Gabbaï. *J. Am. Chem. Soc.*, **124**, 3737 (2002)
54. M.R.Haneline, F.P.Gabbaï. *Z. Naturforsch., Sect. B*, **59**, 1483 (2004)
55. K.I.Tugashov, D.A.Gribanyov, F.M.Dolgushin, A.F.Smol'yakov, A.S.Peregudov, M.Kh.Minacheva, I.A.Tikhonova, V.B.Shur. *Organometallics*, **35**, 2197 (2016)
56. Springer Materials Release 2016 (Dataset ID sd_0541988); HgF2 Crystal Structure https://materials.springer.com/isp/crystallographic/docs/sd_0541988
57. F.M.Dolgushin, A.F.Smol'yakov, K.Yu.Suponitsky, A.V.Vologzhanina, I.V.Fedyanin, S.V.Shishkina. *Struct. Chem.*, **27**, 37 (2016)
58. H.Lee, C.B.Knobler, M.F.Hawthorne. *J. Am. Chem. Soc.*, **123**, 8543 (2001)
59. H.Lee, M.Diaz, C.B.Knobler, M.F.Hawthorne. *Angew. Chem., Int. Ed.*, **39**, 776 (2000)
60. A.A.Zinn, Z.Zheng, C.B.Knobler, M.F.Hawthorne. *J. Am. Chem.* Soc., **118**, 70 (1996)
61. R.G.Pearson. *J. Am. Chem. Soc.*, **85**, 3533 (1963)
62. J.M.Koomen, J.E.Lucas, M.R.Haneline, J.D.Beckwith King, F.Gabbai, D.H.Russell. *Int. J. Mass Spectrom.*, **225**, 225 (2003)
63. K.I.Tugashov, D.A.Gribanyov, F.M.Dolgushin, A.F.Smol'yakov, A.S.Peregudov, I.A.Tikhonova, V.B.Shur. *Organometallics*, **34**, 1530 (2015)
64. F.M.Dolgushin. Doctoral Thesis in Chemical Sciences, INEOS RAS, Moscow, 2018
65. X.Yang, S.E.Johnson, S.I.Khan, M.F.Hawthorne. *Angew. Chem., Int. Ed. Engl.*, **31**, 893 (1992)
66. M.J.Bayer, S.S.Jalisatgi, B.Smart, A.Herzog, C.B.Knobler, M.F.Hawthorne. *Angew. Chem., Int. Ed.*, **116**, 1854 (2004)
67. X.Yang, C.B.Knobler, M.F.Hawthorne. *J. Am. Chem. Soc.*, **114**, 380 (1992)
68. Z.Zheng, X.Yang, C.B.Knobler, M.F.Hawthorne. *J. Am. Chem. Soc.*, **115**, 5320 (1993)

69. Z.Zheng, C.B.Knobler, M.F.Hawthorne. *J. Am. Chem. Soc.*, **117**, 5105 (1995)
70. Z.Zheng, C.B.Knobler, M.D.Mortimer, G.Kong, M.F.Hawthorne. *Inorg. Chem.*, **35**, 1235 (1996)
71. H.Lee, C.B.Knobler, M.F.Hawthorne. *Angew. Chem., Int. Ed.*, **40**, 2124 (2001)
72. K.I.Tugashov, D.A.Gribanyov, F.M.Dolgushin, A.F.Smol'yakov, A.S.Peregudov, Z.S.Klemenkova, O.V.Matvienko, I.A.Tikhonova, V.B.Shur. *Organometallics*, **36**, 2437 (2017)
73. V.B.Shur, I.A.Tikhonova, F.M.Dolgushin, A.I.Yanovsky, Yu.T.Struchkov, A.Yu.Volkonsky, E.V.Solodova, S.Yu.Panov, P.V.Petrovskii, M.E.Vol'pin. *J. Organomet. Chem.*, **443**, C19 (1993)
74. V.B.Shur, I.A.Tikhonova, F.M.Dolgushin, A.I.Yanovsky, Yu.T.Struchkov, A.Yu.Volkonsky, E.V.Solodova, S.Yu.Panov, P.V.Petrovskii, M.E.Vol'pin. *Dokl. Akad. Nauk*, **328**, 339 (1993)
75. M.Yu.Antipin, Yu.T.Struchkov, A.Yu.Volkonsky, E.M.Rokhlin. *Bull. Acad. Sci. USSR, Div. Chem. Sci. (Engl. Transl.)*, **32**, 410 (1983)
76. N.P.Gambaryan, I.V.Stankevich. *Russ. Chem. Rev.*, **58**, 1103 (1989)
77. A.L.Chistyakov, I.V.Stankevich, N.P.Gambaryan, I.A.Tikhonova, V.B.Shur. *Russ. Chem. Bull. (Engl. Transl.)*, **44**, 997 (1995)
78. A.L.Chistyakov, I.V.Stankevich, N.P.Gambaryan, I.A.Tikhonova, V.B.Shur. *Russ. Chem. Bull. (Engl. Transl.)*, **45**, 37 (1996)
79. A.L.Chistyakov, I.V.Stankevich, N.P.Gambaryan, Yu.T.Struchkov, A.I.Yanovsky, I.A.Tikhonova, V.B.Shur. *J. Organomet. Chem.*, **536** – **537**, 413 (1997)
80. M.Ponce-Vargas, A.Munoz-Castro. *J. Phys. Chem. C*, **118**, 28244 (2014)
81. I.A.Tikhonova, F.M.Dolgushin, A.I.Yanovsky, Yu.T.Struchkov, A.N.Gavrilova, L.N.Saitkulova, E.S.Shubina, L.M.Epstein, G.G.Furin, V.B.Shur. *J. Organomet. Chem.*, **508**, 271 (1996)
82. V.N.Tsupreva, O.A.Filippov, F.M.Dolgushin, K.I.Tugashov, A.I.Krylova, V.I.Bragin, I.A.Tikhonova, V.B.Shur, L.M.Epstein, E.S.Shubina. *Russ. Chem. Bull., Int. Ed.*, **57**, 2540 (2008)
83. K.I.Tugashov, D.A.Gribanyov, F.M.Dolgushin, A.F.Smol'yakov, A.S.Peregudov, M.Kh.Minacheva, B.N.Strunin, I.A.Tikhonova, V.B.Shur. *J. Organomet. Chem.*, **747**, 167 (2013)
84. E.S.Shubina, I.A.Tikhonova, E.V.Bakhmutova, F.M.Dolgushin, M.Yu.Antipin, V.I.Bakhmutov, I.B.Sivaev, L.N.Teplitskaya, I.T.Chizhevsky, I.V.Pisareva, V.I.Bregadze, L.M.Epstein, V.B.Shur. *Chem. – Eur. J.*, **7**, 3783 (2001)
85. I.A.Tikhonova, E.S.Shubina, F.M.Dolgushin, K.I.Tugashov, L.N.Teplitskaya, A.M.Filin, I.B.Sivaev, P.V.Petrovskii, G.G.Furin, V.I.Bregadze, L.M.Epstein, V.B.Shur. *Russ. Chem. Bull, Int. Ed.*, **52**, 594 (2003)
86. I.A.Tikhonova, F.M.Dolgushin, K.I.Tugashov, O.G.Ellert, V.M.Novotortsev, G.G.Furin, M.Yu.Antipin, V.B.Shur. *J. Organomet. Chem.*, **689**, 82 (2004)
87. X.Yang, C.B.Knobler, M.F.Hawthorne. *J. Am. Chem. Soc.*, **115**, 4904 (1993)
88. A.A.Zinn, C.B.Knobler, D.E.Harwell, M.F.Hawthorne. *Inorg. Chem.*, **38**, 2227 (1999)
89. L.N.Saitkulova, E.V.Bakhmutova, E.S.Shubina, I.A.Tikhonova, G.G.Furin, V.I.Bakhmutov, N.P.Gambaryan, A.L.Chistyakov, I.V.Stankevich, V.B.Shur, L.M.Epstein. *J. Organomet. Chem.*, **585**, 201 (1999)
90. E.A.Malinina, V.V.Avdeeva, L.V.Goeva, N.T.Kuznetsov. *Russ. J. Inorg. Chem.*, **55**, 2148 (2010)
91. F.M.Dolgushin, K.Yu.Suponitsky, A.F.Smol'yakov, N.A.Shtel'tser, S.V.Osintseva. In *Methods and Applications of Computational Chemistry, MACC-5. Book of Abstracts*. (Kharkiv, 2013). P. 104
92. X.Yang, Z.Zheng, C.B.Knobler, M.F.Hawthorne. *J. Am. Chem. Soc.*, **115**, 193 (1993)
93. H.Lee, C.B.Knobler, M.F.Hawthorne. *Angew. Chem., Int. Ed.*, **40**, 3058 (2001)
94. M.C.Ball, D.S.Brown, A.G.Massey, D.A.Wickens. *J. Organomet. Chem.*, **206**, 265 (1981)
95. I.A.Tikhonova, F.M.Dolgushin, A.I.Yanovsky, Z.A.Starikova, P.V.Petrovskii, G.G.Furin, V.B.Shur. *J. Organomet. Chem.*, **613**, 60 (2000)
96. I.A.Tikhonova, F.M.Dolgushin, K.I.Tugashov, G.G.Furin, P.V.Petrovskii, V.B.Shur. *Russ. Chem. Bull., Ent. Ed.*, **50**, 1673 (2001)
97. I.A.Tikhonova, F.M.Dolgushin, K.I.Tugashov, P.V.Petrovskii, G.G.Furin, V.B.Shur. *J. Organomet. Chem.*, **654**, 123 (2002)
98. J.B.King, M.Tsunoda, F.P.Gabbaï. *Organometallics*, **21**, 4201 (2002)
99. J.B.King, M.R.Haneline, M.Tsunoda, F.P.Gabbaï. *J. Am. Chem. Soc.*, **124**, 9350 (2002)
100. J.Baldamus, G.B.Deacon, E.Hey-Hawkins, P.C.Junk, C.Martin. *Austr. J. Chem.*, **55**, 195 (2002)
101. S.P.Fisher, E.W.Reinheimer. *J. Chem. Crystallogr.*, **43**, 478 (2013)
102. S.P.Fisher, H.R.Krueger Jr., R.H.Groeneman, E.W.Reinheimer. *J. Mol. Struct.*, **1103**, 140 (2016)
103. S.P.Fisher, R.Ramos, R.H.Groeneman, J.W.Kenney III, E.W.Reinheimer. *J. Organomet. Chem.*, **848**, 239 (2017)
104. C.Reichardt. *Solvents and Solvent Effects in Organic Chemistry*. (3rd Edn). (Weinheim: Wiley-VCH, 2003)
105. A.Munoz-Castro, D.MacLeod Carey, R.Arratia-Perez. *J. Phys. Chem. A*, **114**, 666 (2010)
106. I.A.Tikhonova, A.A.Yakovenko, K.I.Tugashov, F.M.Dolgushin, V.V.Novikov, M.Yu.Antipin, V.B.Shur. *Organometallics*, **25**, 6155 (2006)
107. I.A.Tikhonova, F.M.Dolgushin, A.A.Yakovenko, K.I.Tugashov, P.V.Petrovskii, G.G.Furin, V.B.Shur. *Organometallics*, **24**, 3395 (2005)
108. M.R.Haneline, F.P.Gabbaï. *Inorg. Chem.*, **44**, 6248 (2005)
109. I.A.Tikhonova, A.A.Yakovenko, K.I.Tugashov, F.M.Dolgushin, P.V.Petrovskii, M.Kh.Minacheva, B.N.Strunin, V.B.Shur. *Russ. Chem. Bull., Int. Ed.*, **62**, 710 (2013)
110. I.A.Tikhonova, K.I.Tugashov, F.M.Dolgushin, A.A.Yakovenko, P.V.Petrovskii, G.G.Furin, A.P.Zaraisky, V.B.Shur. *J. Organomet. Chem.*, **692**, 953 (2007)
111. A.P.Zaraisky, O.I.Kachurin, L.I.Velichko, I.A.Tikhonova, G.G.Furin, V.B.Shur. *J. Mol. Catal. A: Chem.*, **231**, 103 (2005)
112. M.Tsunoda, F.P.Gabbaï. *J. Am. Chem. Soc.*, **122**, 8335 (2000)
113. M.R.Haneline, R.E.Taylor, F.P.Gabbaï. *Chem. – Eur. J.*, **9**, 5188 (2003)
114. M.R.Haneline, M.Tsunoda, F.P.Gabbaï. *J. Am. Chem. Soc.*, **124**, 3737 (2002)
115. C.N.Burress, M.I.Bodine, O.Elbjeirami, J.H.Reibenspies, M.A.Omary, F.P.Gabbaï. *Inorg. Chem.*, **46**, 1388 (2007)
116. M.A.Omary, R.M.Kassab, M.R.Haneline, O.Elbjeirami, F.P.Gabbaï. *Inorg. Chem.*, **42**, 2176 (2003)
117. T.J.Taylor, C.N.Burress, L.Pandey, F.P.Gabbaï. *Dalton Trans.*, 4654 (2006)
118. M.R.Haneline, J.B.King, F.P.Gabbaï. *Dalton Trans.*, 2686 (2003)
119. K.I.Tugashov, S.M.Yunusov, E.S.Kalyuzhnaya, F.M.Dolgushin, A.S.Peregudov, Z.S.Klemenkova, M.Kh.Minacheva, I.A.Tikhonova, V.B.Shur. *Eur. J. Inorg. Chem.*, 5018 (2019)

120. O.Elbjeirami, C.N.Burress, F.P.Gabbaï, M.A.Omary. *J. Phys. Chem. C*, **111**, 9522 (2007)
121. A.S.Filatov, E.A.Jackson, L.T.Scott, M.A.Petrukhina. *Angew. Chem., Int. Ed.*, **48**, 8473 (2009)
122. A.S.Filatov, A.K.Greene, E.A.Jackson, L.T.Scott, M.A.Petrukhina. *J. Organomet. Chem.*, **696**, 2877 (2011)
123. C.N.Burress, F.P.Gabbaï. *Heteroat. Chem.*, **18**, 195 (2007)
124. C.Burress, O.Elbjeirami, M.A.Omary, F.P.Gabbaï. *J. Am. Chem. Soc.*, **127**, 12166 (2005)
125. M.R.Haneline, F.P.Gabbaï. *C.R. Chimie*, **7**, 871 (2004)
126. R.Castaneda, A.A.Yakovenko, S.Draguta, M.S.Fonari, M.Yu.Antipin, T.V.Timofeeva. *Cryst. Growth Des.*, **15**, 1022 (2015)
127. S.P.Fisher, R.H.Groeneman, E.W.Reinheimer. *J. Coord. Chem.*, **68**, 3589 (2015)
128. R.Castaneda, V.N.Khrustalev, A.Fonari, J.-L.Bredas, Y.A.Getmanenko, T.V.Timofeeva. *J. Mol. Struct.*, **1100**, 506 (2015)
129. R.Castaneda, M.S.Fonari, C.Risko, Y.A.Getmanenko, T.V.Timofeeva. *Cryst. Growth Des.*, **16**, 2190 (2016)
130. S.P.Fisher, E.W.Reinheimer. *J. Chem. Cryst.*, **44**, 123 (2014)
131. T.J.Taylor, F.P.Gabbaï. *Organometallics*, **25**, 2143 (2006)
132. T.J.Taylor, O.Elbjeirami, C.N.Burress, M.Tsunoda, M.I.Bodine, M.A.Omary, F.P.Gabbaï. *J. Inorg. Organomet. Polym.*, **18**, 175 (2008)
133. I.A.Tikhonova, K.I.Tugashov, F.M.Dolgushin, A.A.Yakovenko, B.N.Strunin, P.V.Petrovskii, G.G.Furin, V.B.Shur. *Inorg. Chim. Acta*, **359**, 2728 (2006)
134. M.R.Haneline, F.P.Gabbaï. *Angew. Chem., Int. Ed.*, **43**, 5471 (2004)
135. I.A.Tikhonova, F.M.Dolgushin, K.I.Tugashov, P.V.Petrovskii, M.Yu.Antipin, V.B.Shur. *Russ. Chem. Bull., Int. Ed.*, **53**, 2871 (2004)
136. I.A.Tikhonova, D.A.Gribanyov, K.I.Tugashov, F.M.Dolgushin, A.S.Peregudov, D.Yu.Antonov, V.I.Rosenberg, V.B.Shur. *J. Organomet. Chem.*, **695**, 1949 (2010)
137. M.Fleischmann, J.S.Jones, F.P.Gabbaï, M.Scheer. *Chem. Sci.*, **6**, 132 (2015)
138. M.Fleischmann, C.Heindl, M.Seidl, G.Balázs, A.V.Virovets, E.V.Peresypkina, M.Tsunoda, F.P.Gabbaï, M.Scheer. *Angew. Chem., Int. Ed.*, **51**, 9918 (2012)
139. M.Fleischmann, J.S.Jones, G.Balázs, F.P.Gabbaï, M.Scheer. *Dalton Trans.*, **45**, 13742 (2016)
140. I.A.Tikhonova, D.A.Gribanyov, K.I.Tugashov, F.M.Dolgushin, A.F.Smol'yakov, A.S.Peregudov, Z.S.Klemenkova, V.B.Shur. *Organometallics*, **28**, 6567 (2009)
141. I.A.Tikhonova, D.A.Gribanyov, K.I.Tugashov, F.M.Dolgushin, A.F.Smol'yakov, A.S.Peregudov, Z.S.Klemenkova, V.B.Shur. *ARKIVOC*, (viii), 172 (2011)
142. A.Tikhonova, K.I.Tugashov, F.M.Dolgushin, P.V.Petrovskii, V.B.Shur. *Organometallics*, **26**, 5193 (2007)
143. K.I.Tugashov, D.A.Gribanyov, F.M.Dolgushin, A.F.Smol'yakov, A.S.Peregudov, Z.S.Klemenkova, I.G.Barakovskaya, I.A.Tikhonova, V.B.Shur. *Organometallics*, **38**, 2910 (2019)
144. I.A.Tikhonova, K.I.Tugashov, F.M.Dolgushin, A.A.Korlyukov, P.V.Petrovskii, Z.S.Klemenkova, V.B.Shur. *J. Organomet. Chem.*, **694**, 2604 (2009)
145. M.Tsunoda, F.P.Gabbaï. *J. Am. Chem. Soc.*, **125**, 10492 (2003)
146. A.Burini, J.P.Fackler, R.Galassi, T.A.Grant, M.A.Omary, M.A.Rawashdeh-Omary, B.R.Pietroni, R.J.Staples. *J. Am. Chem. Soc.*, **122**, 11264 (2000)
147. R.F.W.Bader. *Atoms In Molecules. A Quantum Theory*. (Oxford: Clarendron Press, 1990)
148. M.Tsunoda, M.Fleischmann, J.S.Jones, N.Bhuvanesh, M.Scheer, F.P.Gabbaï. *Dalton Trans.*, **45**, 5045 (2016)
149. J.Wang, R.S.Price, G.Leem, J.Jiang, K.A.Abboud, K.S.Schanze. *Chem. Mater.*, **30**, 5968 (2018)
150. R.Salles, B.Abécassis, E.Derat, D.Brouri, A.Bernard, Q.Zhang, A.Proust, C.Desmarets, G.Izzet. *Inorg. Chem.*, **59**, 2458 (2020)
151. A.Karmakar, M.M.A.Soliman, G.M.D.M.Rúbio, M.F.C.G.Silva, A.J.L.Pombeiro. *Dalton Trans.*, **49**, 8075 (2020)
152. I.Alkorta, J.Elguero, A.Frontera. *Crystals*, **10**, 180 (2020)
153. A.A.Korlyukov, Yu.V.Nelyubina. *Russ. Chem. Rev.*, **88**, 677 (2019)
154. A.M.Reilly, R.I.Cooper, C.S.Adjiman, S.Bhattacharya. *Acta Crystallogr., Sect. B*, **B72**, 439 (2016)
155. C.A.Gunawardana, C.B.Aakeröy. *Chem. Commun.*, **54**, 14047 (2018)
156. A.A.Mohamed. *Coord. Chem. Rev.*, **254**, 1918 (2010)
157. V.N.Tsupreva, A.A.Titov, O.A.Filippov, A.N.Bilyachenko, A.F.Smol'yakov, F.M.Dolgushin, D.V.Agapkin, I.A.Godovikov, L.M.Epstein, E.S.Shubina. *Inorg. Chem.*, **50**, 3325 (2011)
158. A.A.Titov, O.A.Filippov, A.N.Bilyachenko, A.F.Smol'yakov, F.M.Dolgushin, V.K.Belsky, I.A.Godovikov, L.M.Epstein, E.S.Shubina. *Eur. J. Inorg. Chem.*, 5554 (2012)
159. A.A.Titov, O.A.Filippov, E.A.Guseva, A.F.Smol'yakov, F.M.Dolgushin, L.M.Epstein, V.K.Belsky, E.S.Shubina. *RSC Adv.*, **4**, 8350 (2014)
160. R.Galassi, S.Ricci, A.Burini, A.Macchioni, L.Rocchigiani, F.Marmottini, S.M.Tekarli, V.N.Nesterov, M.A.Omary. *Inorg. Chem.*, **52**, 14124 (2013)
161. J.Zheng, Z.Lu, K.Wu, G.-H.Ning, D.Li. *Chem. Rev.*, **120**, 9675 (2020)